

The relationship between Neogene dinoflagellate cysts and global climate dynamics

Jamie L. Boyd¹, James B. Riding^{2*}, Matthew J. Pound³, Stijn De Schepper⁴, Ruza F. Ivanovic¹,
Alan M. Haywood¹ and Stephanie E.L. Wood⁵

¹School of Earth and Environment, University of Leeds, Woodhouse Lane, Leeds LS1 9JT, UK

²British Geological Survey, Environmental Science Centre, Keyworth, Nottingham NG12 5GG, UK

*jbri@bgs.ac.uk

³Department of Geography and Environmental Science, Northumbria University, Newcastle upon
Tyne NE1 8ST, UK

⁴Uni Research Climate, Bjerknes Centre for Climate Research, PO Box 7801, N-5020 Bergen,
Norway

⁵Department of Animal and Plant Sciences, University of Sheffield, Western Bank, Sheffield S10
2TN, UK

Key Words: dinoflagellate cysts; global distributions; Neogene; palaeoclimate; palaeoecology;
palaeotemperature

Abstract

The Neogene Period (23.03–2.59 Ma) underwent a relatively gradual cooling trend, culminating in
present day climate conditions. Neogene studies have provided important information for
understanding how modern patterns of atmospheric and oceanic circulation developed, and how
they may relate to environmental change. Here we use a newly created global database of Neogene

dinoflagellate cysts (the Tertiary Oceanic Parameters Information System - TOPIS) to investigate how dinoflagellate cysts recorded the cooling of Neogene surface marine waters on a global scale. Species with warm and cold water preferences were determined from previously published literature and extracted from the database. Percentages of cold water species were calculated relative to the total number of species with known temperature preferences from each site and compared throughout the Neogene at differing latitudes. Globally, dinoflagellate cysts indicate that cooling was not uniform at all latitudes and that the rate of cooling was not constant. Cooling predominantly occurred in the middle to high latitudes from the Pliocene onwards. The cooling trend indicated by Neogene dinoflagellate cysts generally agrees with other established environmental proxies such as foraminifera. This also demonstrates the use of dinoflagellate cysts in determining temperature change on both extended temporal and wide geographical scales.

Introduction

The Neogene Period (23.03–2.59 Ma) was significantly warmer than the present, and is considered to have been the ‘making of the modern world’ (Potter and Szatmari, 2009; Pound et al., 2012a). This is because many important changes occurred that resulted in our current climate. These include alterations to marine gateways (Osbourne et al., 2014; Sijp et al., 2014; Montes et al., 2015), the growth of high latitude continental scale ice sheets (Dowsett et al., 2016; De Schepper et al., 2014; 2015; Brierley and Fedorov, 2016; Stein et al., 2016) and the development of major mountain belts (Raymo and Ruddiman, 1992; Spicer et al., 2003; Graham, 2009; Ruddiman, 2013; von Hagke et al., 2014; Fauquette et al., 2015). All these phenomena combined to change the oceanic and the atmospheric circulations and hence, together with carbon dioxide (CO₂) fluctuations, altered the climate from the relatively warm and ice-free Paleogene, gradually cooling during the Neogene, to the significantly colder temperatures of the Pliocene and Pleistocene (Pearson and Palmer, 2000; Zachos et al., 2001; 2008; Kürschner et al., 2008; Salzmänn et al., 2008; 2013; Pound et al., 2012a;

Herbert et al., 2016; Pound and Salzmann, 2017). The general cooling trend throughout the Cenozoic was occasionally interrupted by several relatively short-lived warm intervals. The principal examples of these are the Mid Miocene Climatic Optimum (MMCO) between 17 and 15 Ma (Wright et al., 1992; Flower and Kennett, 1993; 1994; Zachos et al., 2001; 2008; Herbert et al., 2016), and the mid Piacenzian Warm Period (mPWP) between 3.264 and 3.025 Ma (Haywood et al., 2002; 2013; Robinson et al., 2011). Nevertheless, the longer-term global cooling continued, and eventually culminated in the establishment of large ice sheets in the high northern latitudes (e.g. Shackleton et al. 1984, Jansen et al. 1988, Balco and Rovey 2010) and the decrease of deep sea temperatures by over 10 °C as well as the decrease of surface temperatures of 6 °C (Zachos et al., 2001; 2008; Hansen et al., 2013; Herbert et al., 2016).

1.1 Dinoflagellate cysts

Dinoflagellate cysts are increasingly being used as a temperature proxy (Head, 1994; 1997; Versteegh and Zonneveld, 1994; De Schepper et al., 2009; 2011; 2015; Warny et al., 2009; Schreck and Matthiessen, 2013; Verhoeven and Louwye, 2013; Hennissen et al., 2014). Dinoflagellates are an extant group of unicellular eukaryotic phytoplankton; they are typically marine and planktonic in habit, and are important primary producers (Taylor et al., 2008). Their organic walled resting cysts are most common in marine sediments. Dinoflagellate cysts are normally composed of the biopolymer dinosporin (Fensome et al., 1993; Versteegh et al., 2012; Bogus et al., 2012; 2014). Wall composition differs between taxa, probably related to feeding strategy (Bogus et al., 2014). While the wall of autotrophic dinoflagellate cysts is generally resistant to oxidation, heterotrophic taxa can be degraded and destroyed by oxidation (Zonneveld et al., 1997). Nevertheless, they are useful proxies for palaeoenvironmental reconstruction because they have global distributions, are abundant and diverse, occur continuously in the fossil record from the mid Triassic onwards and their distribution is controlled by different environmental parameters (Marret and Zonneveld, 2003; Zonneveld et al., 2013). Modern biogeographical distributions are related to parameters such as

nutrient levels, salinity, sea ice cover and temperature (Harland, 1983; Rochon et al., 1999; Marret and Zonneveld, 2003; Radi and de Vernal, 2008; Bonnet et al., 2012; de Vernal et al., 2013; Limoges et al., 2013; Zonneveld et al., 2013a). The environmental preferences of modern dinoflagellate cysts can be compared to the Neogene fossil record of extant taxa, making it possible to infer palaeoenvironmental conditions (Brinkhuis et al., 1998; Sluijs et al., 2005; Masure and Vrielynck, 2009; De Schepper et al., 2011; Woods et al., 2014). However, in deeper time there is an increase in extinct species, which limits the use of nearest living relative concept (Head, 1996, 1997; Wijnker et al. 2008; De Schepper et al. 2015).

Deciphering the palaeoecology of extinct dinoflagellate cyst species is achieved by comparing assemblages with proxies for absolute sea-surface temperatures (De Schepper et al., 2011; Hennissen et al. 2017). This has demonstrated that extant species had comparable sea surface temperature ranges in the Pliocene, and that sea surface temperature ranges can be estimated for extinct species. Multivariate analysis can be used to identify temperature sensitive species (Versteegh, 1994; Hennissen et al. 2017). Furthermore latitudinal, and hence climatological, preferences can be inferred from palaeogeographical maps (Masure and Vrielynck, 2009; Masure et al., 2013).

This is the first global study of Neogene marine environmental cooling using dinoflagellate cysts as a temperature proxy. This investigation of an important group of phytoplankton over an interval of >20 myr provides an unprecedented view of the marine realm worldwide. As such, we are able to answer three key questions: can dinoflagellate cysts be used to determine global cooling in the Neogene; was the cooling during the Neogene uniform at all latitudes; and was the rate of cooling uniform across the whole Neogene?

2. Material

The data used come from the newly developed Tertiary Oceanic Parameters Information System (TOPIS), a Microsoft Access - ArcGIS database containing public domain, peer-reviewed literature on Neogene dinoflagellate cysts. Overall 275 publications are included, totalling 500 globally distributed sites. The database was produced by compiling and entering data from published studies into three forms: 'main', 'layer' and 'flora'. In the 'main' form, key information (bibliographical references, location and approximate age of the samples, dating methods and sample preparation method) is entered with the option to include information on the nearest country and/or ocean basin to the sample site (Figure 1). The 'layer' form contains stratigraphical information such as lithology, formation/member and the detailed age model (Figure 1). This format allows more precise ages to be given by breaking down the overall cores/outcrop sections into smaller divisions. Therefore, once the third and final form (the 'flora' form) is completed, the dinoflagellate cysts can be shown as part of a smaller and more constrained age range, representing individual assemblages (Figure 1). The 'flora' form documents the individual dinoflagellate cyst taxa and, if available, their relative abundance as a percentage of the total dinoflagellate cyst assemblage (Figure 1). The new database makes it possible to analyse and compare the results of published research on a global scale, and enables global analysis of the development of Neogene oceans and dinoflagellate cyst biogeography over long time scales.

Main ID	79	Lit ID	44	Lit ID2		Site Name	Davis Strait, Offsh
Country	Greenland	Ocean	Labrador Sea	Age Max	13.82	Age Min	1.81
Latitude	63.6	Palaeo latitude	62.197				
Longitude	-53.819	Palaeo longitude	-49.173				
Dating method	Based on foraminifer	Sample prep.	HCl - HF -briefly oxidised by weak solution of nitric acid - washed in potassium hydroxide				
Quality	4						
Layer ID	607	Main ID	79	Formation		Age Max	11.6
Oceanic Settings	Not given.	Sediment	Horizontally stratified			Age Min	7.25
Ocean Setting ID	None given	Sediment ID	Sand	Depth (m)	1781.6		
Notes							
Flora_ID	7169	Layer_ID	607	Taxon ID	15		
Abundance		Notes					

Figure 1: Example screen shot from the Microsoft Access database; Tertiary Oceanic Parameters Information System (TOPIS) showing the three key forms: Main, Layer and Flora.

2.1 Construction of the database

The John Williams Index of Palaeopalynology (JWIP; Riding et al., 2012) was interrogated in order to ensure that the coverage was as comprehensive as possible. The JWIP is the most comprehensive reference catalogue on palaeopalynology in the world, and contains 23,350 references as of February 2012 (Riding et al., 2012). Whilst it is inevitable that a small amount of literature may have been missed, confidence can be placed in TOPIS to have included the vast majority of available published material on Neogene dinoflagellate cysts. Data published after 2014 have not been included in the analysis in order to facilitate the investigation in a consistent manner.

The diverse nature of the literature used in the TOPIS database means that multiple dating techniques are incorporated into the synthesis. The majority of published dinoflagellate cyst assemblage age assessments were derived biostratigraphically, typically using calcareous nannofossils, foraminifera and palynomorphs, with fewer based on diatoms, mammals, molluscs,

magnetostratigraphy or radiometric methods. The dating method in each paper is given a confidence value termed Quality (Figure 1) between one (high) and five (low) in order to estimate the reliability of the dating in a semi-quantitative fashion. In general, studies that utilised multiple dating methods or radiometric dating were assigned Quality values of one or two. Publications using biostratigraphy were assigned a Quality value of either three or four depending on the number of fossil groups used. Whereas, Quality values of five were assigned to publications where only vague dating information was provided.

Because TOPIS contains a diverse range of publications, each with its own different aims and objectives, the resolution of the individual assemblages is variable. Age ranges of individual dinoflagellate cyst assemblages vary from less than 0.001 Myr to over 25 Myr. The majority of the assemblages (1394 assemblages) are dated to within one or two stages of the Neogene and assemblages with a maximum and minimum age range spanning longer than two stages (267 assemblages) were excluded from the analysis to avoid using poorly constrained data that may influence the results. An additional 442 assemblages were included that had estimated age ranges spanning less than one million years. A maximum of two stages were chosen as TOPIS contains assemblages that have a relatively high dating resolution, but happen to span the boundary between two stages.

During the production of this compilation, the date of publication was carefully noted due to the evolving nature of the geological time scale. If the time scale was not explicitly stated in a publication, it was assumed that the most up to date iteration at the time of issue was used. Any changes between pre-2012 versions and Gradstein et al. (2012) were noted. Where necessary, the estimated age ranges of the assemblages were emended to represent the current geological time scale (Gradstein et al., 2012). The majority of the publications affected were those that did not give quantitative age controls, and only provided the stage name(s) as the estimated age range of the assemblages. The major change to the calibration of the Neogene recently was the transition of the

Gelasian from the Pliocene into the Pleistocene, effectively shortening the Pliocene to 2.58 Ma (Gibbard et al., 2010). This meant that the age estimates of any publications published prior to 2010, which dated assemblages as Pliocene, were altered to 5.333–1.806 Ma rather than the shorter 5.333–2.59 Ma range of the Pliocene in the modern geological time scale.

Site locations are given as latitude and longitude coordinates, either taken directly from the published literature (when provided), or projected (from the location figure provided) onto a map using online cartographical resources such as Google Earth. If the location was not provided with sufficient resolution, the notes section of the database states that it is approximate. Sites are rotated to their palaeoposition (Figure 2) using a plate rotation model (Pound et al., 2011; Hunter et al., 2013) that is compatible with the underlying palaeogeographies of Markwick et al. (2000).

2.2 Taxonomy, reworking and treatment of dinoflagellate assemblages

The rationale of the TOPIS database follows that of the Tertiary Environmental Vegetation Information System (TEVIS; Salzmann et al., 2008; 2013; Pound et al., 2011; 2012a) and the Bartonian/Rupelian dinoflagellate cyst database of Woods et al. (2014). As in these previously published databases, TOPIS undertakes little reinterpretation of the primary data in order to allow rapid construction and interpretation of large-scale trends (Salzmann et al., 2008; 2013; Pound et al., 2011; 2012a; Woods et al., 2014). The large amount of data collated, and the broad scale of the analysis, helps mitigate against any problematic taxonomy (Woods et al., 2014).

A consistent dinoflagellate cyst taxonomy based upon Fensome et al. (2008) was used to identify and disregard synonyms. Obvious synonyms were combined/disregarded, and where doubt existed, species were checked against published photographic plates or were not included in any analysis.

Synonyms that are combined that are not included in the current version of Dinoflag2 include:

Barssidinium pliogenicum and *Barssidinium wrennii* (De Schepper et al., 2004); *Dapsilidinium pseudocolligerum* and *Dapsilidinium pastielsii* (Mertens et al., 2014) and *Operculodinium tegillatum* and *Operculodinium antwerpensis* (Louwye and De Schepper, 2010). These were all recently noted

by Williams et al. (2017). Subspecies were treated at the species level; for example, *Achomosphaera andalousiensis* subsp. *andalousiensis* was entered in the database as *Achomosphaera andalousiensis*. Several of the species included in the analysis of this paper have been grouped into complexes (supplementary data); for example, *Spiniferites elongatus* and *Spiniferites frigidus* have been grouped due to gradations in morphology (Rochon et al., 1999) as were *Batiacasphaera micropapillata* and *Batiacasphaera minuta* (Schreck and Matthiessen, 2013). Taxa not defined to species level and questionably assigned species were also not included in any analysis.

The stratigraphical range for each species in TOPIS was checked, and if reworking of a species was suspected, the species in question was removed from that record. Reworked species were established by the original authors indicating a reworked species and/or by checking with previously published range charts produced for the Neogene (e.g. de Verteuil and Norris, 1996; Munsterman and Brinkhuis, 2004; De Schepper and Head, 2008). There is a possibility that some reworked species were still included. However, according to Woods et al. (2014), reworking is unlikely to bias any results due to the large quantity of data analysed, combined with limited evidence of reworking in younger sediments (Mertens et al., 2009; Verleye and Louwye, 2010).

Published dinoflagellate cyst assemblages can be presented as either presence/absence of taxa (e.g. Londeix and Jan du Chene, 1998; Louwye et al., 2000), categorically (e.g. between a range of relative abundances; Head, 1989, McCarthy and Mudie, 1996), as raw abundance counts (e.g. Pudsey and Harland 2001; Louwye et al., 2007) or as relative abundance counts (e.g. Richerol et al., 2012; Shreck et al., 2013). In addition, several different counting techniques were used in the literature compiled herein, for example *Spiniferites* spp. or *Spiniferites/Achomosphaera*. Consequently, it was necessary to transform all data into the lowest common form: presence/absence of taxa in order to maximise the geographical and temporal extent of the dataset from TOPIS and to enable identification of large scale trends in dinoflagellate cyst biogeography through the Neogene. Whilst this necessarily loses

some of the fine details of abundance variations with regional environmental changes (Marret and Zonneveld, 2003), the focus of this paper is to identify the global scale change.

2.2.1 Preservation/sample preparation technique

The preservation of dinoflagellate cysts can be affected by oxidation, causing decay and poor preservation (de Vernal and Marret, 2007). Oxidation of dinoflagellate cysts can occur naturally and during sample preparation, particularly in older publications, when reagents such as hydrogen peroxide, nitric acid or Schultze's Solution were added to remove residual fine organic material (Riding and Kyffin-Hughes, 2004). Oxidation particularly affects heterotrophic species (e.g. *Brigantedinium* spp.), which are less resistant, and often results in their complete or partial destruction (Marret, 1993; Head, 1996; Zonneveld et al., 1997; 2001; Hopkins and McCarthy, 2002). By contrast, autotrophic species (G-cysts) such as *Impagidinium* spp. are less sensitive to oxidation (Marret and Zonneveld, 2003). This means that the method used for sample preparation must be carefully chosen as some techniques will selectively remove the more oxidation-prone taxa from the assemblage (Marret, 1993; Mudie and McCarthy, 2006).

The distribution of heterotrophic species is mainly controlled by the presence of nutrients, and thus it is likely that both cold and warm water species will be equally affected by any biasing due to sample preparation methods. If nutrient availability and oxidation are the main controlling influences on the presence and distribution of heterotrophic taxa, rather than temperature (Bockelmann and Zonneveld, 2007), it explains the lack of heterotrophs included amongst the list of species with known temperature preferences (Figure 3 and supplementary data A). Because of these factors, the data compiled herein were not filtered by the sample preparation technique used.

2.2.2 Transport

Dinoflagellate cysts behave as silt sized particles (Dale, 1983; Kawamura, 2004) and, like other microfossil groups, can be transported both vertically through the water column and laterally with ocean currents. This means that there is a possibility that the location at which the fossil was found

may not represent the environmental conditions of their original habitat. (Dale, 1996; de Vernal and Marret, 2007). Several studies have investigated the effects of vertical and lateral movements of dinoflagellate cysts through the water column by comparing cyst assemblages in the water column to the collection of cysts in the underlying sediments (e.g. Harland and Pudsey, 1999; Zonneveld and Brummer, 2000; Pospelova et al., 2008). These studies indicate that the transport of cysts is only a minor factor in the distribution of cysts and is likely to be a local influence only. Experiments in both laboratories and in the oceans, demonstrate that dinoflagellate cysts sink through the water column relatively rapidly (by several metres per day), which can increase to hundreds of metres per day if they are incorporated into faecal pellets or marine snow (Zonneveld and Brummer, 2000).

In our global scale study, transport does not bias the interpretations. Firstly, transport is a process affecting an entire assemblage, meaning that selective transport of only cool water (or warm water) species is very unlikely. Secondly, the modern biogeographical distribution of cool water species accurately reflects the sea surface temperature distribution in the global oceans (Figure 4i, 4j). Both points, together with the modern observations from sediment traps, suggest that transport in the modern oceans is not a major issue when interpreting the relationship of Cold Water Species (CWS) and Warm Water Species (WWS) in a global dataset.

2.3 Dinoflagellate cysts as a temperature proxy

Due to a limited number of dinoflagellate cyst species with a known absolute temperature range and a lack of abundance data, this study is limited to presenting relative temperature change rather than quantifiable temperatures (Marret and Zonneveld, 2003; Zonneveld et al., 2013a). Species that are constrained to certain temperatures are often regarded as only being abundant in such temperature regimes and rarely outside of them. This means that when using presence and absence data, rather than abundance data, the presence of an individual CWS does not necessarily rule out warm water conditions.

Not only is the distribution of dinoflagellate cysts related to prevailing sea surface temperature, they can also respond to salinity, nutrient availability and sea ice cover (Marret and Zonneveld, 2003; Zonneveld et al., 2013a). Temperature and nutrient availability (phosphate and nitrate concentrations) are thought to be the most important controlling variables (Marret and Zonneveld, 2003; Zonneveld et al., 2013a). For example, in areas of upwelling or river discharge, there is often an increase in the concentration of dinoflagellate cysts due to enhanced nutrient availability (Crouch et al., 2003). Without abundance data, it is difficult to determine the location of upwelling systems and river outlets, and care must be taken to interpret results in light of local phenomenon such as the upwelling of colder, nutrient rich waters.

3. Methods

Dinoflagellates and their cysts make excellent temperature proxies, and as such, numerous publications provide evidence of their temperature preferences (Head, 1997; Marret and Zonneveld, 2003; Wijnker et al., 2008; De Schepper et al., 2009; Schreck et al., 2013; Zonneveld et al., 2013a). The supplementary data (A) presents an updated synthesis of literature from which the temperature preference for each dinoflagellate cyst was obtained. Both modern and palaeontological studies were used to ascertain Neogene dinoflagellate cyst temperature preferences. Temperature categories used in the literature include: tropical, warm-temperate to tropical, temperate, cool-temperate and subpolar, but were simplified in this study into Warm Water Species (WWS) and Cold Water Species (CWS). Our WWS group contains 48 species and includes species within the warm-temperate to tropical categories. The CWS consists of 11 species belonging to the cool-temperate to polar categories (Figure 3; supplementary data A). Sites with any of these species present were extracted from TOPIS for use in this analysis (Figure 2; supplementary data B).

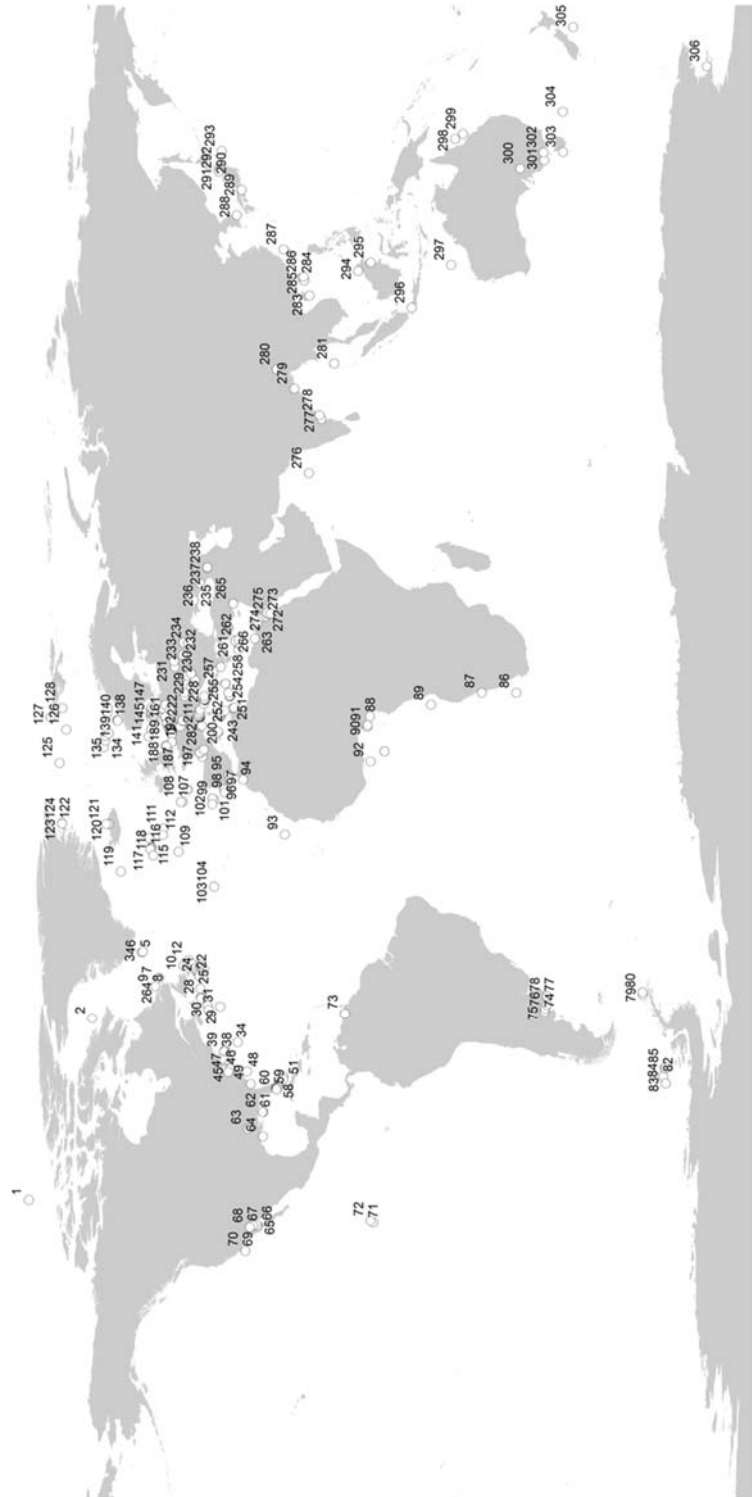


Figure 2: Distribution of all the Neogene records used in this study; the sites are plotted at their modern latitude and longitude, and references are provided in supplementary information B.

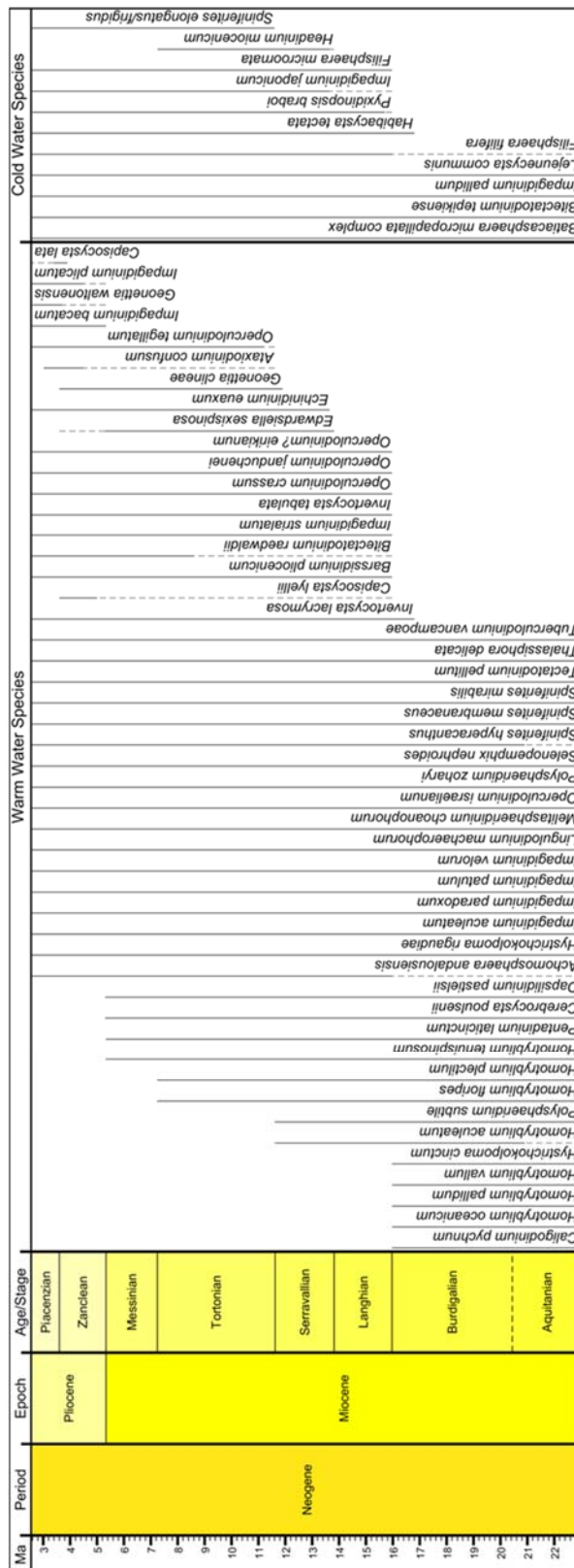


Figure 3: Age ranges of the Neogene dinoflagellate cyst species with known temperature preferences used in this study. Dashed lines represent ages when species are known to have lived, but are not present in the datasets used in this study. References pertaining to temperature preferences are provided in the Supplementary data A.

This resulted in a dataset of 733 records (Figure 2; supplementary data B). The records are from 306 sites (183 publications) and as some sites contain several records of different ages, they have palaeo-latitudes and -longitudes that change through time. A record is defined as one or more dinoflagellate cyst species, with a known temperature preference, occurring at a location with a specific age range. The percentage of CWS, relative to the total number of species with known temperature preferences in each record, was calculated and plotted in ArcGIS 10.4. For the purposes of plotting the data, records were grouped by geological stage and plotted using their palaeo-latitudes and palaeo-longitudes (Salzmann et al., 2013; Pound et al., 2012a; Pound and Salzmann, 2017). The mean percentage of CWS was calculated for each stage (Figure 6a and b) as well as for each 5° latitudinal bin (Figure 7a-i) to understand the change in surface temperature over the Neogene at different latitudes. As the majority of the data are located in the Northern Hemisphere, much of the analysis ignores the Southern Hemisphere. This is an unfortunate limitation that will be addressed as the literature expands to include more Southern Hemisphere study sites.

Our TOPIS fossil database was compared against the modern dinoflagellate cyst world atlas compiled by Zonneveld et al. (2013b). In the latter database, 33 WWS and 10 CWS were recorded. Seventeen of the WWS and five of the CWS are also found in the Neogene, with the remaining species restricted to the modern or Quaternary oceans. After removing records that had no species with known temperature preferences, the modern database was left with a remaining 1,784 records. Cosmopolitan species were considered to have no known temperature preferences as they are not informative for this type of analysis.

4. Results

4.1 Early Miocene (23.03–15.97 Ma)

Only 20% of the records in both the Aquitanian and Burdigalian (Figure 4a, b) had any CWS present, and, with the exception of two records northeast of South America (between 5 and 10° N), no CWS

were found between zero and 25° N (Figures 4a, b, 5). Yet these records off South America contain the highest percentage of CWS relative to WWS in the Northern Hemisphere (25%; *Batiacasphaera micropapillata* complex).

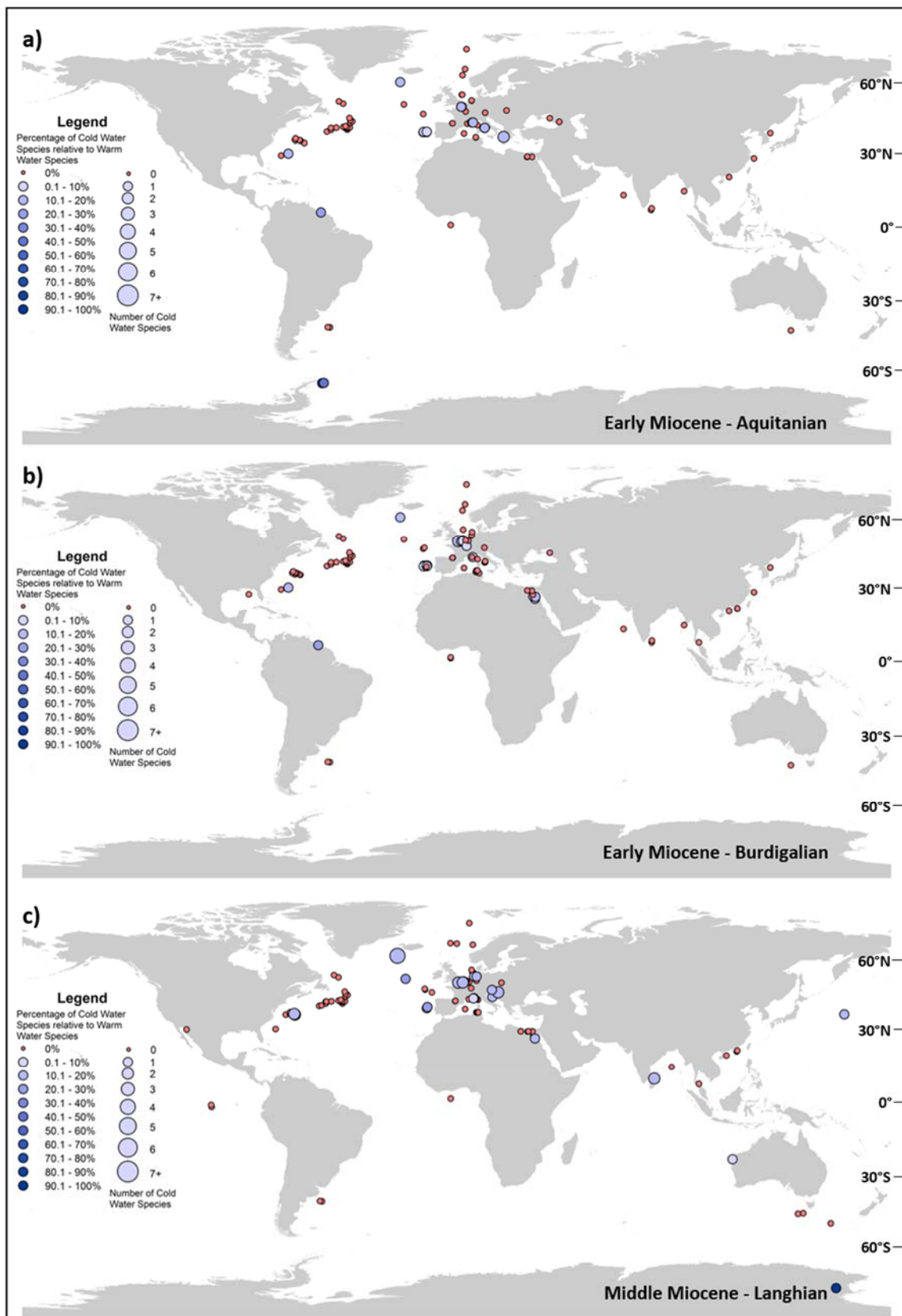
In this study, the *Batiacasphaera micropapillata* complex is defined as a CWS, but they can be found in low quantities at lower latitudes (Schreck and Matthiessen, 2013). This highlights the importance of providing abundance data because without it, it is unclear whether the *B. micropapillata* complex made up a higher percentage of the assemblage (indicating cooler waters), or were present in low abundances.

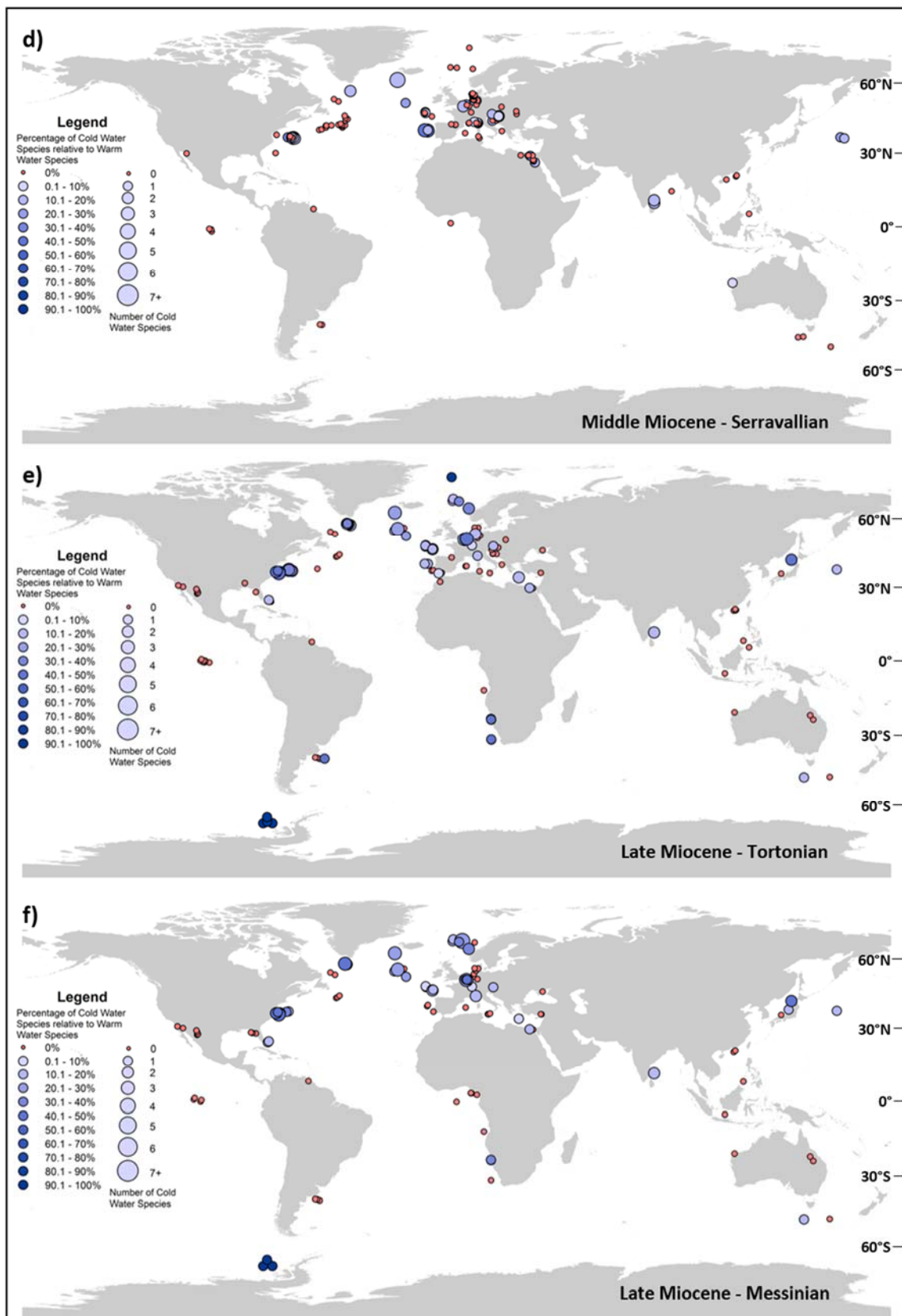
The highest percentage of CWS in the Southern Hemisphere is between 60 and 65° S, off the Antarctic Peninsula, where two records have CWS percentages of 50 and 100%. Globally both the Aquitanian and Burdigalian have low mean percentages of 4 and 3% respectively (Figure 6a), although when exclusively using data from the Northern Hemisphere, the mean percentages are 2 and 3% respectively (Figure 6b). The mean percentage of CWS in each five degree latitude bin ranges from zero to 11% for both stages (Figure 7a, b).

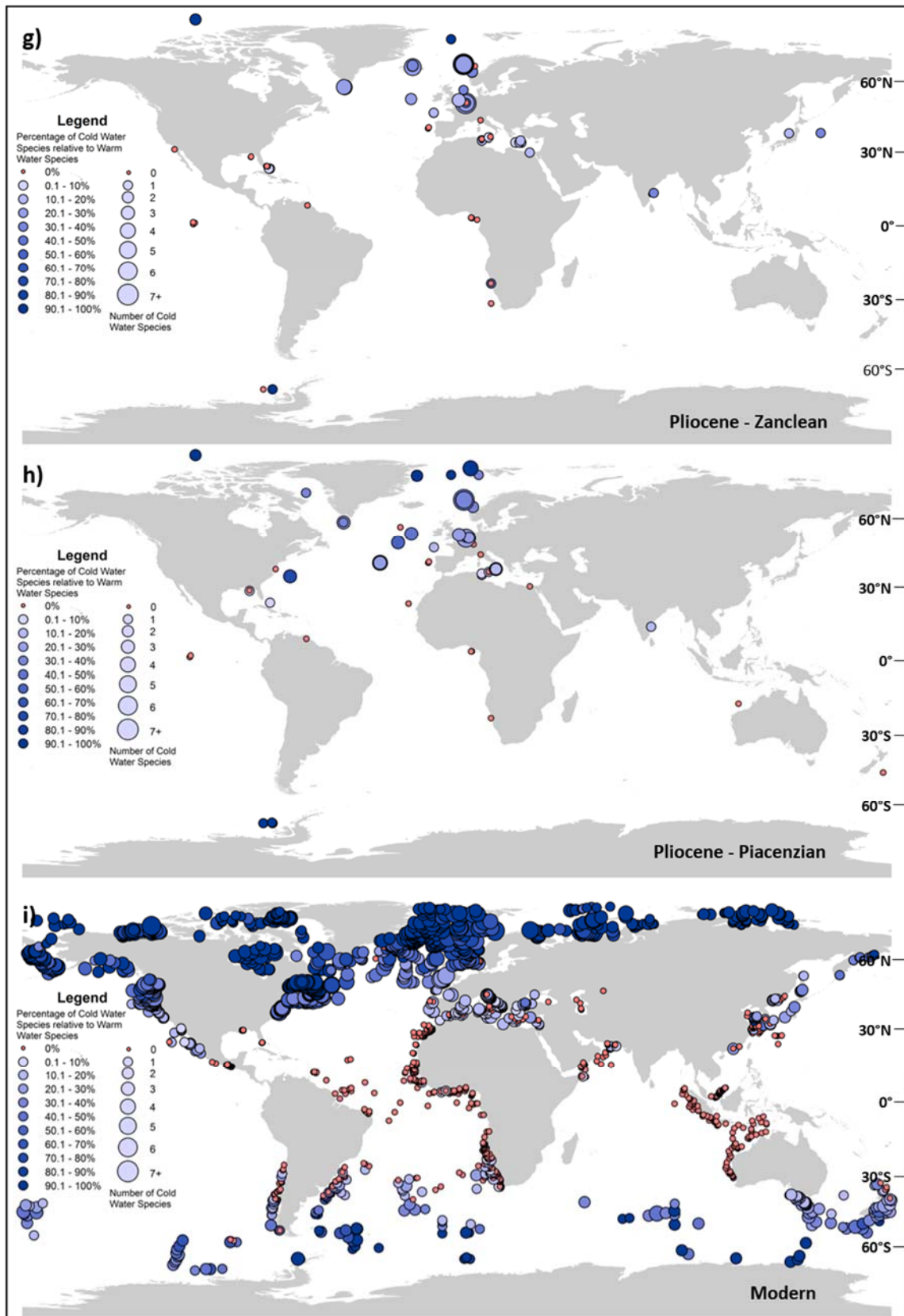
4.2 Mid Miocene (15.97–11.62 Ma)

The mean percentage of CWS (relative to WWS) for each five degree latitude bin ranges from zero to 18% for both the Langhian and Serravallian (Figure 7c, d), and globally the mean percentage is 4 and 5% (Figure 6a) respectively (3 and 6% for just the Northern Hemisphere; Figure 6b). The proportion of records with CWS present increased, compared with the Early Miocene (24 and 31% for the Langhian and Serravallian respectively; Figure 4c, d). Unlike in the Aquitanian and Burdigalian, CWS appeared in three records off the east coast of India (10–15° N; *Batiacasphaera micropapillata* complex and *Bitectatodinium tepikiense*) and are also seen in the West Pacific (20%, 35–40° N). Between 40 and 45° N the proportion of CWS increased from mean values of 0.2% in the Burdigalian to 1.8% in the Langhian to 5.3% in the Serravallian (Figure 7b-d). Central Europe in particular

328 experienced an increase in the proportion of CWS relative to WWS during the Mid Miocene (40–55°
329 N; Figures 4c, d, 5a).







332

333

334

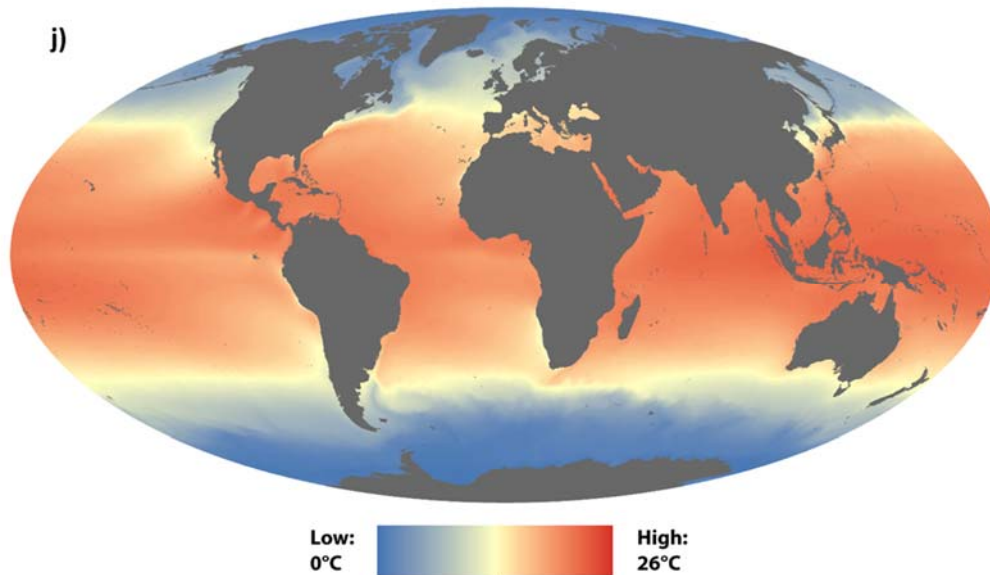


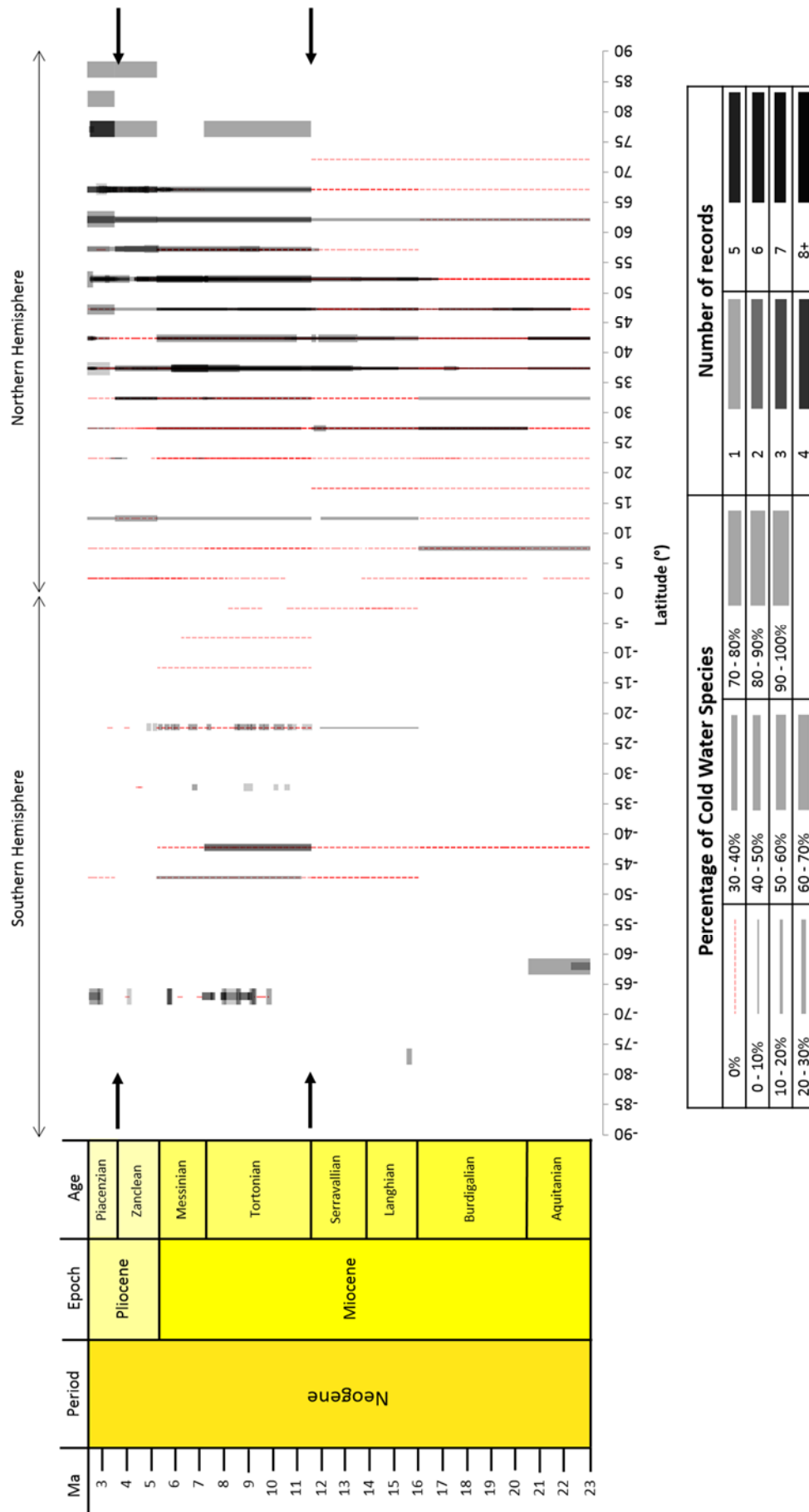
Figure 4: Distribution of dinoflagellate cyst records in (a) Aquitanian, (b) Burdigalian, (c) Langhian, (d) Serravallian, (e) Tortonian, (f) Messinian, (g) Zanclean, (h) Piacenzian and the (i) modern (from Zonneveld et al., 2013b). (j) Mean annual sea surface temperature observed between 2009 and 2013 (from NASA's Ocean Color database: <http://oceancolor.gsfc.nasa.gov>; NASA Ocean Biology OB.DAAC; 2014). For a-i, records are plotted at their palaeo-latitude and -longitudes. Size of the points represents the number of Cold Water Species (CWS) present in each record. The colour of the points represents the percentage of CWS relative to the total number of species with known temperature preferences present in each record. Darker shades represent higher percentages of CWS. Small red circles represent records that only contain Warm Water Species.

4.3 Late Miocene (11.62–5.333 Ma)

In the Late Miocene over half of the records contain CWS (Figure 4e, f), and the mean percentage of CWS (relative to WWS) in each latitudinal bin has a much larger range than for the Mid Miocene, between 0 and 27% (Figure 7e, f). One latitudinal bin (in the Tortonian; 75–80° N) is comprised of only CWS (Figures 5a, 7e). Globally the mean percentage of the Tortonian is 19% and the Messinian is 12% (Figure 6a). However, when using just data from the Northern Hemisphere the mean percentage is 11% and 10% for the Tortonian and Messinian respectively (Figure 6b). The high

latitudes in particular (50–65° N) had an increase in the proportion of CWS relative to WWS with the introduction of CWS to records off the coast of Norway (up to 33% CWS) and off the coast of Japan (17% CWS; Figure 4e, f). One of the more significant differences between the Tortonian and the rest of the Neogene is the number of records in the Southern Hemisphere, which is substantially higher in the Tortonian than for any of the other stages (Figure 5a). The additional records appear off the Antarctic Peninsula (CWS percentages range from 50 to 100%), and off the west coast of South Africa (CWS percentages of 100%; *Bitectatodinium tepikiense*). The presence of these CWS (*Bitectatodinium tepikiense* and *Ataxiodinium choane*) is related to the initiation of the Benguela upwelling in the Late Miocene that produced cold nutrient rich waters at the surface (Siesser, 1980; Diester-Haass et al., 1990; Robert et al., 2005; Heinrich et al., 2011).

a)



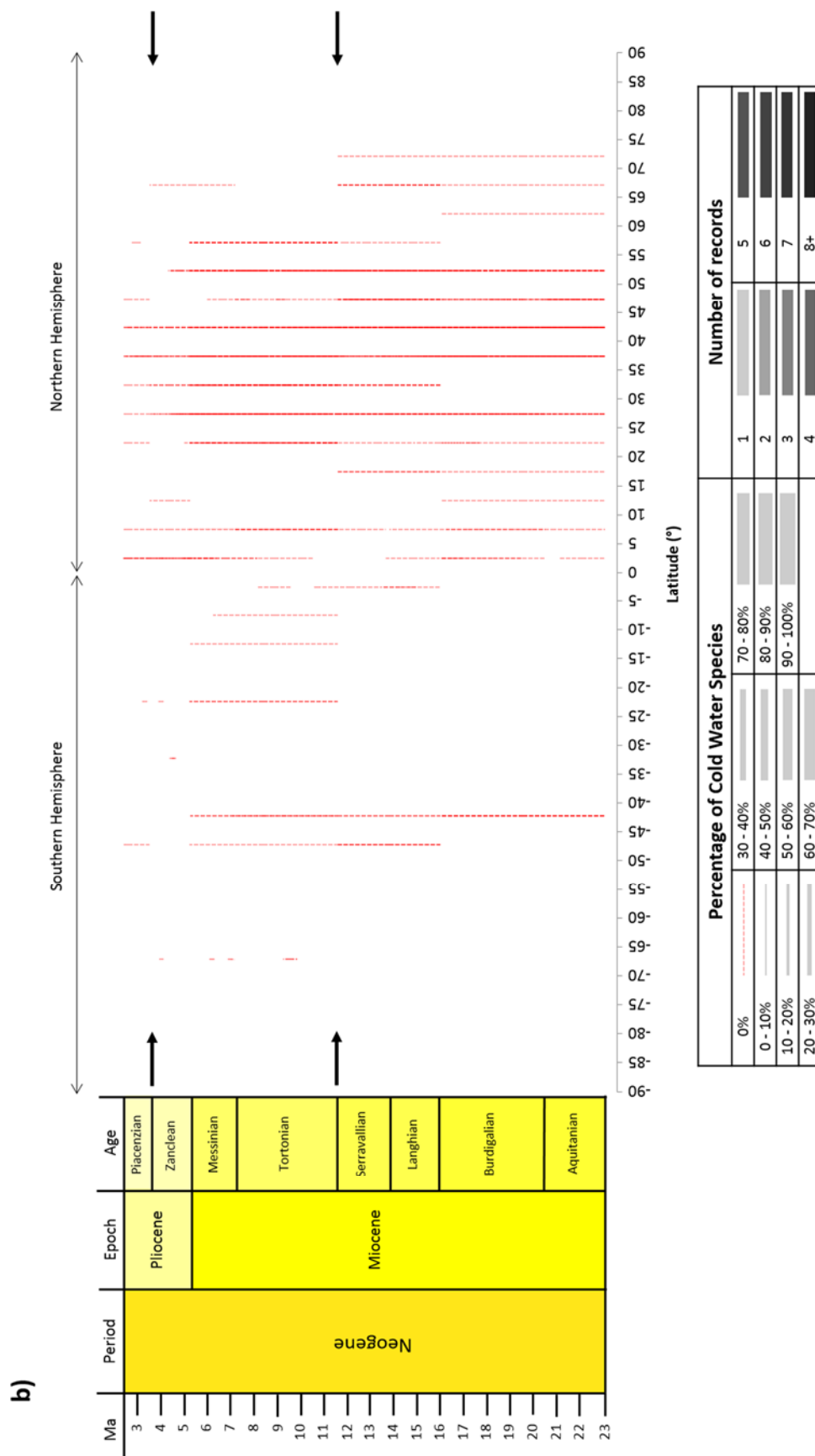


Figure 5: Dinoflagellate cyst data for the entire Neogene is divided into latitudinal bins spanning five degrees. There are consistently more data for the Northern Hemisphere than the Southern Hemisphere. For each record, the percentage of

CWS was calculated relative to the number of species with known temperature preferences. The percentage of CWS is displayed and is represented by the horizontal thickness of the line. The shading of the lines represents the number of records present within each latitudinal bin. Dashed red lines represent records with no CWS. Figure 5a represents all records and Figure 5b contains only those records with no CWS present. Arrows indicate the two main periods of cooling. To help explore uncertainties, the number of records found within each latitudinal bin is represented by the shading. The darker the shading, the more data are present, and therefore the more reliable the signal is likely to be.

4.4 Pliocene (5.333–2.588 Ma)

In the Zanclean and Piacenzian (Figure 4g, h), the mean percentages of CWS between 0 and 45° N are all under 7%. The one exception is between the latitudes of 10 to 15° N, which has a mean CWS percentage of 17%. The mean percentages of CWS north of 55° N are all over 20%, and above 75° N they are 87% or higher. Globally, the mean percentages of the Zanclean and Piacenzian are 17 and 28%, which are very similar to the values calculated when using data exclusively from the Northern Hemisphere (17 and 27%). The proportion of records with CWS present attained as high as 71% in the Piacenzian and the proportion of CWS making up each record increases particularly between the Zanclean and the Piacenzian. For example, in the Piacenzian records, CWS percentages of 11 to 15% appear in the Mediterranean. Records where all of the species with known temperatures preferences are CWS can be found north of Canada, east of Greenland and west of Svalbard.

4.5 Modern surface sediments

Data for surface sediments comes from Zonneveld et al. (2013b). There is a significantly higher number of sites in the modern than for the Neogene and a broad global distribution is achieved (Figure 4i). As in the Neogene, there are fewer records for the Southern Hemisphere compared to the Northern Hemisphere, and the Indian and Pacific oceans are also under-represented (Figure 4i). For the majority of ocean basins, most of the records come from the coasts, and relatively few come from deeper and more oceanic regions. Sites that are composed only of CWS are common in higher latitudes in both the Southern and Northern Hemispheres. In the lower latitudes, species with known temperatures are nearly all WWS. Between 20° N and 20° S, there are only four records (out

of 377) that contain any CWS. Three of these are found off the west coast of Africa and the fourth is off the east coast of Africa, all have CWS percentages under 10%. Records composed entirely of CWS are common above and below 45° N and 45° S, respectively. Asymmetry occurs either side of the North Atlantic. Records where all of the species with known temperature preferences are CWS reach as far south as 42° N on the western edge of the North Atlantic, but only as far south as 56° N on the eastern side. This likely stems from the presence of the North Atlantic Current, which transports warm water to the higher latitudes of the northeast North Atlantic Ocean.

The global mean percentage of CWS for surface sediments is substantially higher (38%) than for the stages of the Neogene (Figure 6a), as is the mean percentage when comparing just the Northern Hemisphere (43%; Figure 6b). When calculating the mean percentage of CWS for just those latitudes where data is present for the Neogene, the mean percentage of CWS is still high at 34% (Figure 6b). In the modern (Figure 5i), between 0 and 35° N, the mean percentages of CWS relative to WWS are all under five percent, which quickly rises to 50% and above north of 45° N (Figure 7i).

An example of where the spread of data influences the results can be seen in the modern map (Figure 4i). There are a very high number of records (95) in the Gulf of Saint Lawrence, on the east coast of Canada, contributing 33% of all the records between 45 and 55° N. In 72 of these records, all the species with known temperature preferences are CWS (mostly *Spiniferites elongatus* and *Islandinium minutum*). The remaining 13 records from the Gulf of Saint Lawrence have CWS percentages between 50 and 83%. These results indicate that the Gulf of Saint Lawrence is particularly cold compared to the rest of the oceans at this latitude (Figure 7i). It is a small, restricted basin that receives a large quantity of freshwater and has limited exchange with the open ocean (Long et al., 2015). The only open ocean water source is through the Belle Isle Strait, bringing cool Labrador Sea water into the Gulf. However, the majority of the cool waters form *in situ* during the winter season (Banks, 1966; Saucier et al., 2003). The plethora of sites reflecting the cool water Gulf of Saint Lawrence microclimate produces a noticeable feature in the modern. In the modern 45–55°

418 N latitudinal bins, the mean percentage of CWS relative to WWS is significantly higher than it was in
419 the 40–45° N latitudinal bin (Figure 7i). If the 95 records from the Gulf of Saint Lawrence are
420 removed from the analysis, this step like change seen at roughly 45° N is no longer present,
421 providing a clear example of how a large number of records in a small region can alter the global
422 signal, and demonstrating why it is preferable to have an even spatial coverage of data.

423

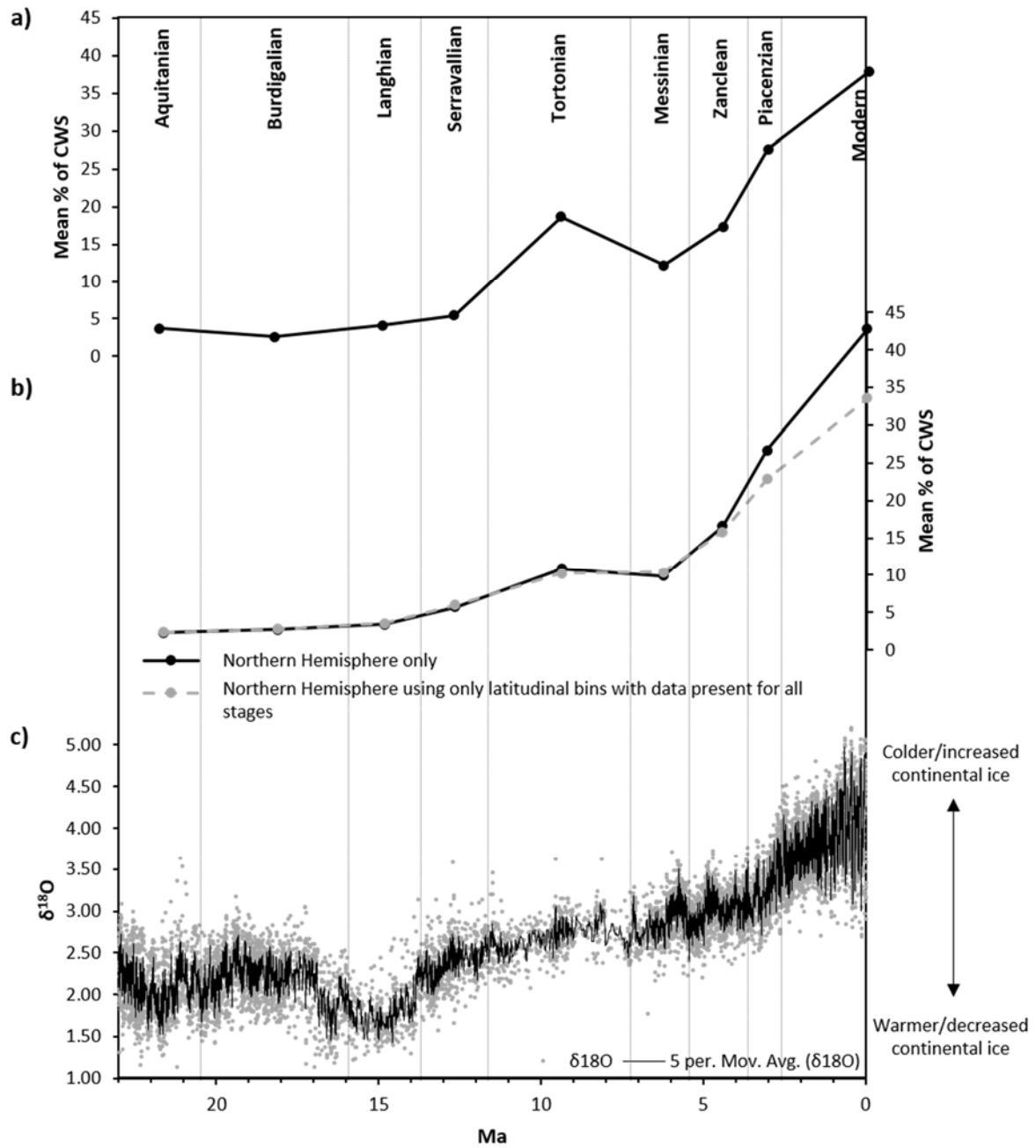


Figure 6: Mean percentages of Cold Water Species (CWS) of dinoflagellate cysts for each stage for (a) all records, (b) only records from the Northern Hemisphere and using only the latitudinal bins (in the Northern Hemisphere) where data are available for all stages. (c) Benthic $\delta^{18}\text{O}$ compilation (Zachos et al., 2001; 2008) demonstrating cooling through the Neogene to present for comparison with the mean percentage of CWS.

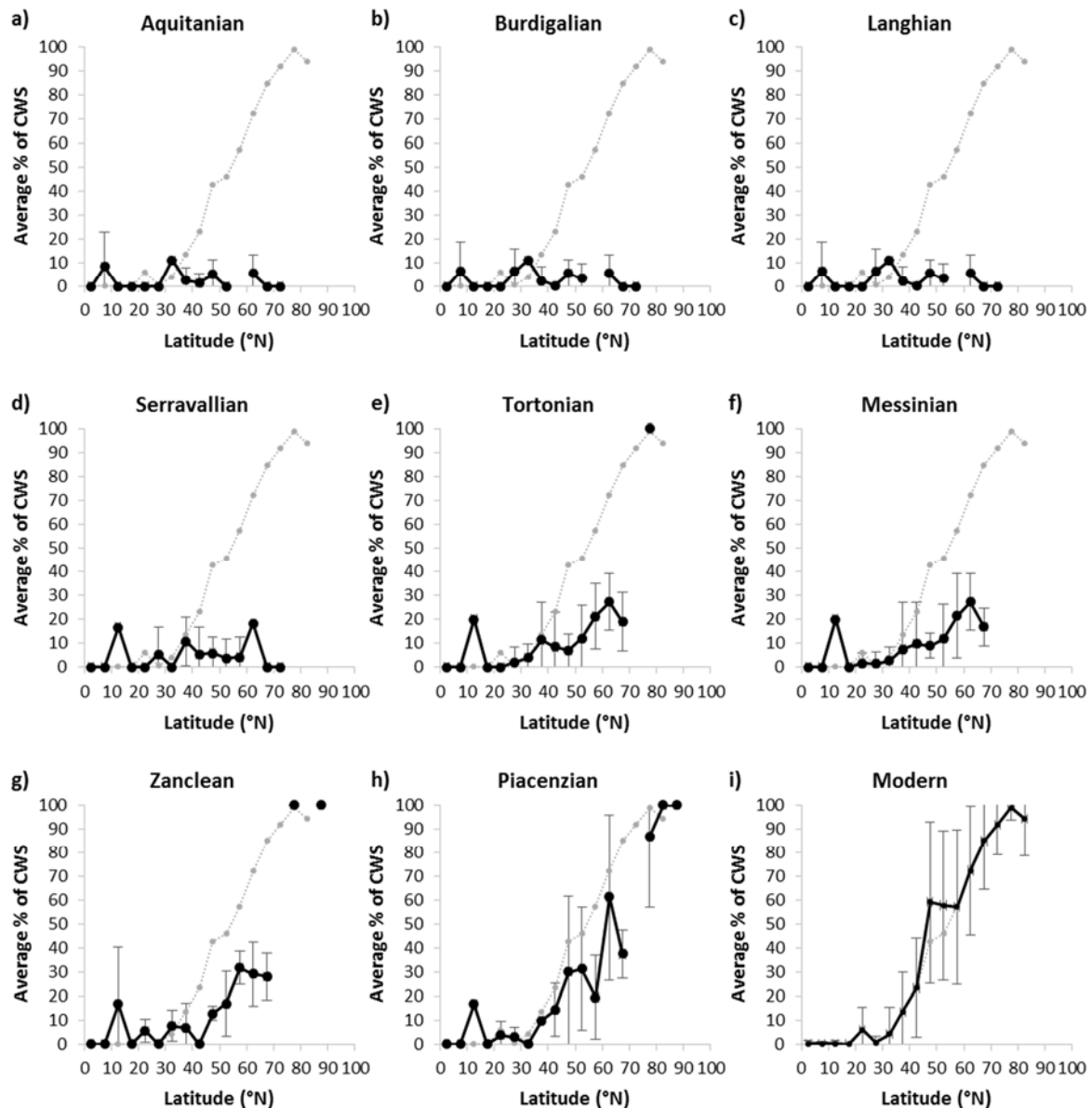


Figure 7: The mean percentage of Cold Water Species (CWS) of dinoflagellate cysts relative to the total number of species present with known temperature preferences for each five degree latitudinal bin. (a) Aquitanian, (b) Burdigalian, (c) Langhian, (d) Serravallian, (e) Tortonian, (f) Messinian, (g) Zanclean, (h) Piacenzian and (i) the modern. The grey lines in panels (a) to (h) represent modern data (without data from the Gulf of Saint Lawrence) for comparison. For the modern data were replotted without data points from the Gulf of St. Lawrence (grey dashed line), a densely sampled region, to investigate sampling bias (see Subsection 5.3.3). Error bars represent the standard deviation.

4.6 The pull of the recent and the latitudinal biodiversity gradient

Temperature preferences of dinoflagellate cysts are better known for those species that are either extant or most recently became extinct. This phenomenon is known as ‘the pull of the recent’ and

was originally conceived for diversity studies, particularly in the Cenozoic (Raup, 1979; Jablonski et al., 2003). If the pull of the recent was affecting the results, it is possible that the increasing number of CWS in successively younger stages is due to a better understanding of the temperature preferences of dinoflagellate cysts. It is for this reason that the main analysis compared the proportion of CWS to WWS, rather than the absolute number of CWS present (Figures 3, 4). However, with the exception of the Early Miocene, which has the fewest species with known temperature preferences (Figure 8; five CWS and 30 WWS), the pull of the recent effect does not seem to have influenced the rest of the Neogene, and the number of species found in each stage is highest for the Tortonian (Figure 8). It is also worth noting that when the percentage of CWS and WWS (present in each stage) is calculated relative to each other (Figure 8), the percentage of CWS in each stage increases through the Neogene with the cooling temperatures. As the pull of the recent presumably affects CWS and WWS equally, suggesting the CWS and WWS ratio is unaffected (Figure 8; black dashed line), the increase in the proportion of CWS relative to WWS through the Neogene is due to the cooling climate.

Throughout the Neogene, there is a significantly higher number of WWS than CWS (Figure 8). This is likely due to the latitudinal biodiversity gradient where the warmer, lower latitudes have a higher diversity than the cooler, higher latitudes. This phenomenon has been observed in the geological record for at least the last 30 Myr (Crame, 2001; Mittelbach et al., 2007; Mannion et al., 2014). This relatively low species richness of CWS is an enduring feature of the dinoflagellate cyst record, and hence does not affect our interpretations. There are fewer localities in the most northerly/southerly latitudes, which may have potentially led to higher numbers of WWS compared to CWS. However, as this is consistent throughout the Neogene, it is unlikely to bias our results.

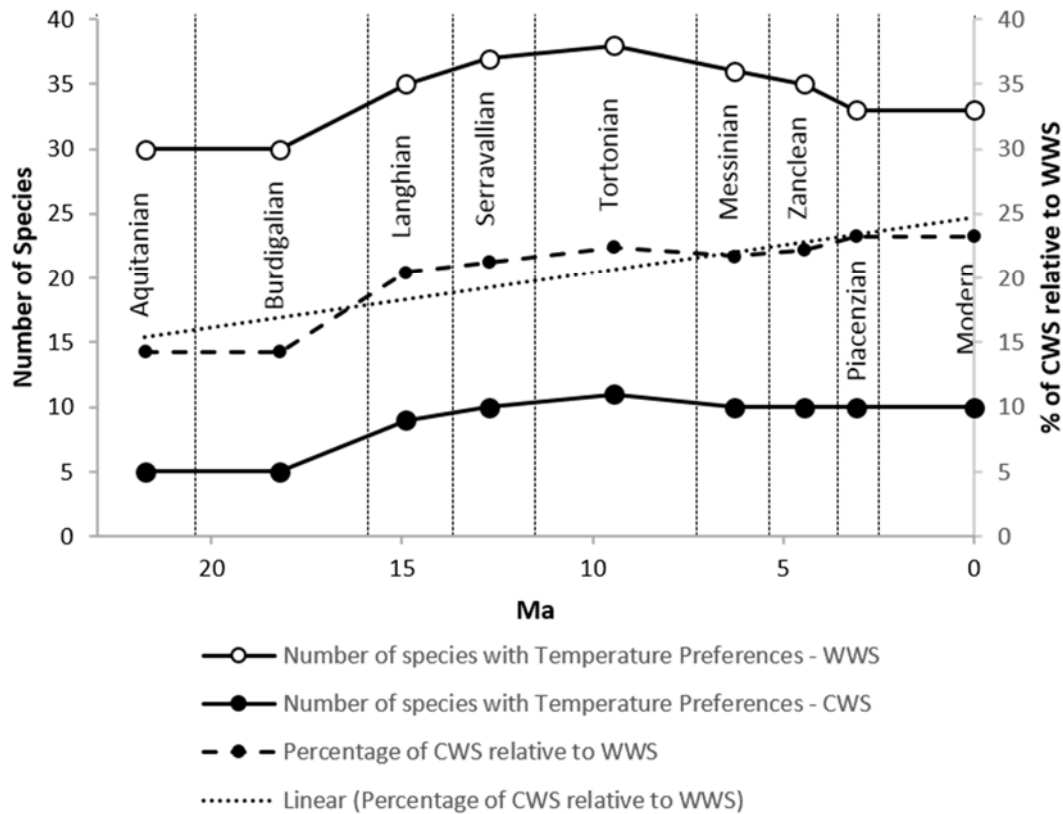


Figure 8: The number of dinoflagellate cyst species with warm or cold water preferences for each stage (red and blue lines; plotted on the left axis) and the percentage of Cold Water Species (CWS) that make up the total number of species with known temperature preferences for each stage (black line; plotted on the right axis). The data were obtained by counting the number of species in each stage from the range chart in Figure 3.

5. Discussion

5.1 The Early Miocene (23.03–15.97 Ma)

Immediately prior to the Miocene, the Mi-1 event (23.13 Ma, Abels et al., 2005) in the benthic oxygen isotope record shows a shift to cooler bottom waters and/or increased ice accumulation on Antarctica (Zachos et al., 2001; Billups and Schrag, 2002; Wilson et al., 2013; Beddow et al., 2016). Whilst evidence for ice sheets in the Northern Hemisphere is uncertain, sea-ice was present in the Arctic (Moran et al., 2006). Whereas, ice accumulation at one or potentially both poles indicates a relatively cool climate, the mean CWS percentage of 2% for the Aquitanian and 3% for the Burdigalian is more indicative of globally warmer oceans (Figure 4a, b). With the exception of

occurrences off the Antarctic Peninsula, the CWS occurrences of the Aquitanian and Burdigalian are not at the high latitudes and can be compared to the occurrence of CWS in the modern Mediterranean Sea (Zonneveld et al., 2013b). The low numbers of CWS during the Early Miocene indicates that the latitudinal temperature gradient was considerably more stable than at present (Figure 7a, b). This was previously suggested by Nikolaev et al. (1998) from a compilation of foraminifera and oxygen isotope data. The Early Miocene was not an interval of sustained warmth; alkenone data from the Paratethys Sea shows a 2–3 °C cooling between 18.4 and 17.8 Ma (Grunert et al., 2014). These rapid climate changes are not detected in the present study due to low dating resolution in many dinoflagellate cyst studies (Figure 9).

5.1.1 Sampling and time/age bias

The average age range of the records for each stage is variable (Figure 9). The records from the Aquitanian and Burdigalian have the longest age range (4.7 and 4.4 Myr respectively), and the Zanclean and the Piacenzian records have the shortest age ranges (0.9 and 0.8 Myr respectively). This is partly due to the nature of the dating. For example, much of the literature dates each record to within a stage or in some cases, to the nearest sub-epoch (i.e. the Early Miocene). Thus, the records of the longer stages, such as the Burdigalian (spanning 4.47 Myr) have a higher average age range, while the Piacenzian (the shortest stage of the Neogene; 1.02 Myr in duration) has a much lower average record length. Unfortunately, this means that any evidence of short scale events affecting dinoflagellate cysts, such as the MMCO and the mPWP, is lost in this study. However, it is still possible to interpret long-term changes and, in the future, it should be possible to interrogate global dinoflagellate cyst biogeography for higher-resolution studies of climate and environmental change.

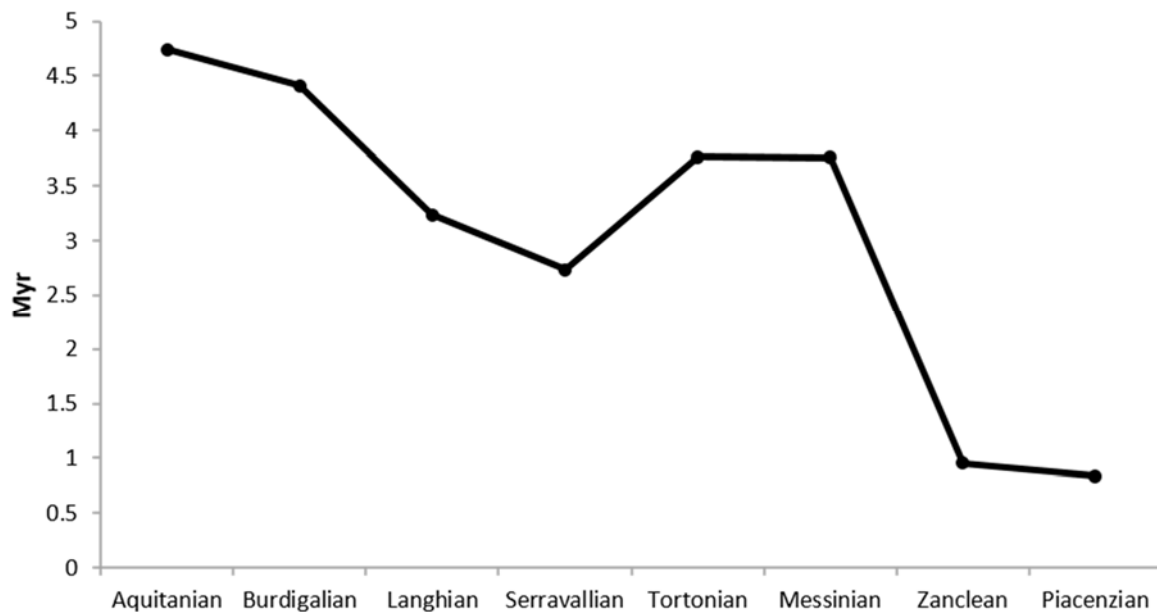


Figure 9: The average age range of dinoflagellate cyst records for each stage. Generally, temporal resolution of the data increases in stages of a shorter duration as much of the data are dated to within a stage.

5.2 The Mid Miocene (15.97–7.25 Ma)

The Mid Miocene is both an interval of sustained global warmth (MMCO; 17–14.5 Ma) and one of step-like global cooling at Mi-3a, Mi-3b, Mi-4 and Mi-5 (ca. 14–11.6 Ma) (Savin et al., 1975; Shackleton and Kennett, 1975; Zachos et al., 2001; Böhme, 2003; You et al., 2009; Quaijtaal et al., 2014). This general pattern of a warm Langhian and a cooling Serravallian is recorded in the percentage of CWS in each stage (Figure 6). Towards the end of the Early Miocene, benthic $\delta^{18}\text{O}$ values rapidly decreased, suggesting a reduction in continental ice and a global warming event (Zachos et al., 2001; 2008). The warming event culminated in the MMCO, which was a period of global warmth between 17 and 15 Ma (Savin et al., 1975; Shackleton and Kennett, 1975; Zachos et al., 2001; Böhme, 2003; You et al., 2009) and resulted in the tropical climate zone having a much greater latitudinal extent, abundant precipitation and decreased seasonality (Böhme, 2003; Bojar et al., 2004; Kroh, 2007; Pound et al., 2012a). Even though mean global temperatures of the MMCO were more than 3°C higher than today (Pagani et al., 1999; Kürschner et al., 2008; You et al., 2009; Foster et al., 2012), evidence for such a warming is not obvious in this study, and the dinoflagellate

514 cyst cooling trend does not follow that of Zachos et al. (2001; 2008; Figure 6a-c). This is likely due to
515 a lack of high-resolution data in the TOPIS database, which is unable to resolve the MMCO and
516 preceding warming (Figure 9).

517 The lack of warming observed during the MMCO in TOPIS may be due to a lack of abundance data.
518 For example, Warny et al. (2009) detected the MMCO in Antarctica by a 2000-fold abundance
519 increase of just two species. These authors associated the peak in productivity with increased
520 meltwater runoff from the elevated temperatures of the MMCO (Warny et al., 2009). This
521 demonstrates how routine reporting of abundance data in the literature would enhance our ability
522 to understand Neogene climate trends.

523 What is evident from the database, is that a cooling trend occurred between the Langhian and the
524 Serravallian resulting in a slight increase in the percentage of CWS (Figure 6a, b). Whilst the slight
525 increase in the percentage of CWS is apparent, it is not as characteristic as the step-like cooling
526 demonstrated by benthic $\delta^{18}\text{O}$ values during the Serravallian (Figure 6c; Quaijtaal et al., 2014). The
527 lack of a major cooling event indicated by the dinoflagellate cyst record may again be due to the
528 temporal resolution not detecting the relatively short steps in Miocene cooling. Instead, the
529 Serravallian consistently has higher percentages of CWS than preceding stages, indicating that
530 dinoflagellate cysts did respond to the cooling, but not uniformly in the surface waters at all
531 latitudes. This may relate to the asymmetrical nature of the cooling; the latitudinal temperature
532 gradient steepened first in the Southern Hemisphere during the Serravallian in response to the
533 expansion of Antarctic ice sheets (Pound et al., 2012a). Whilst the Northern Hemisphere (in the
534 North Atlantic region at least) maintained a shallower gradient possible in response to the onset of
535 the warm Gulf Stream ocean current (Denk et al., 2013).

536 While the benthic $\delta^{18}\text{O}$ values significantly increased in the Serravallian, and less in the Tortonian,
537 the dinoflagellate cyst record (Figure 6a-c) demonstrates the opposite. Thus, a more significant
538 cooling is indicated in the Tortonian as opposed to the Serravallian. This might suggest a time-

averaged response of dinoflagellate cysts to the step-like cooling of the Serravallian, or that the surface waters cooled at a different rate to the deep waters. Global biome reconstructions also demonstrate that the cooling was more pronounced between the Serravallian and the Tortonian, than the Langhian and the Serravallian (Pound et al., 2012a). This may reflect a growth of ice sheets during the Serravallian suggesting that the increase in deep water $\delta^{18}\text{O}$ values is a combination of cooling and ice accumulation (Badger et al., 2013; Knorr and Lohmann, 2014). Whereas the Late Miocene did not lead to any additional permanent ice, but indicates continued global cooling (Herbert et al., 2016). In addition, vegetation records (Pound et al., 2012a) demonstrate that the Southern Hemisphere cooled prior to the Northern Hemisphere, and as the majority of the records used in this study are from the Northern Hemisphere, this could be a further explanation for the delayed response of the dinoflagellate cysts to the signal produced by the benthic $\delta^{18}\text{O}$ values (Zachos et al., 2001; 2008).

During the Langhian the Central American Seaway (CAS) shoaled, potentially preventing deep water exchange from around 15 Ma (Montes et al., 2015). Whilst no impacts are evident in the dinoflagellate cyst records most proximal to the CAS, it is important to note that there are currently no dinoflagellate cyst records in TOPIS for the Caribbean during the Mid Miocene (Figure 4). This shoaling or closure would have modified ocean circulation and modelling results have shown that this warms the Northern Hemisphere (Brierly and Federov, 2016). This is consistent with the low numbers of CWS dinoflagellate cysts in the high latitudes of the Northern Hemisphere (Figure 4). The closure of the CAS during the Langhian would have promoted heat transport into the North Atlantic. It would also have tempered the global cooling of the post-MMCO climate as seen in Northern Hemisphere floras (Denk et al., 2013) and strengthened the asymmetrical latitudinal temperature gradient (Pound et al., 2012a).

5.3 The Late Miocene (11.62–5.33 Ma)

The Late Miocene, though still significantly warmer than the present, was considerably cooler than the Mid Miocene (Pound et al., 2012a; Utescher et al., 2015). This is reflected in the increased percentage of, and wider biogeographical distribution of, CWS dinoflagellate cysts (Figures 4, 5). The Tortonian (11.62–7.25 Ma) was characterised by warmer and more humid conditions than today (Bruch et al., 2006; Pound et al., 2011). Mean annual temperatures were between 14 and 16 °C in northwest Europe (Donders et al., 2009; Pound et al., 2012b; Pound and Riding, 2016). Furthermore, the Cenozoic global cooling trend, which resumed at the end of the MMCO, continued (Zachos et al., 2001). However, benthic $\delta^{18}\text{O}$ values demonstrated that the cooling was more gradual for the Tortonian compared to the Serravallian, assuming that there was no additional ice sheet growth (Figure 6c; Zachos et al., 2008). This cooling affected the presence of cold water dinoflagellate cysts, and the mean percentage of CWS reached 10% in the Tortonian (Figure 6b).

The majority of CWS occurrences are in the Northern Hemisphere (Figure 4). This is a clear sampling bias due to the lack of Neogene dinoflagellate cyst records from the Southern Hemisphere (Figure 4). The dinoflagellate cyst record is consistent with global vegetation records that show a cooler, more seasonal, biome distribution in the Northern Hemisphere in the Tortonian, than during the Serravallian (Pound et al., 2012a). Furthermore, pollen-based temperature reconstructions from New Zealand demonstrate Southern Hemisphere cooling immediately after the MMCO (Prebble et al., 2017). The percentage of CWS in the Tortonian in the mid to high latitudes increased, while the percentage in the low latitudes remained similar to the values for the Early and Mid Miocene (Figures 7a-e). The Tortonian was also the earliest stage to have all dinoflagellate cysts with known temperature tolerances being CWS at 75–80° N. This indicates substantial high latitude cooling by this time during the Neogene, which is consistent with proxies for extensive seasonal sea ice in the Arctic during the Tortonian (Stein et al., 2016). The increase in the percentage of CWS in the higher latitudes compared with the low latitudes reflects that tropical regions during the Miocene remained at similar temperatures, whereas the high latitudes cooled (Nikolaev et al., 1998; Williams et al.,

2005; Steppuhn et al., 2006; Herbert et al., 2016). This effect caused the latitudinal temperature gradient to steepen throughout the Late Miocene and Pliocene in the Northern Hemisphere (Nikolaev et al., 1998; Crowley, 2000; Fauquette et al., 2007; Pound et al., 2012a). This temperature decrease in the high latitudes was described by Nikolaev et al. (1998), who demonstrated a 4–6 °C increase in the latitudinal temperature gradient between 10 and 5 Ma. Cooling of the mid to high latitude surface waters during the Late Miocene is also reflected in the alkenone sea surface temperature reconstructions, which demonstrate that temperatures reduced to near modern conditions between 7 and 5.4 Ma (Herbert et al., 2016). Near modern temperatures during the Tortonian are not indicated by Arctic surface water temperatures, dinoflagellate cysts, faunal distributions or global vegetation records (Pound et al., 2012a; Utescher et al., 2015; Azpelicueta and Cione, 2016; Stein et al., 2016; Prebble et al., 2017).

Global temperatures continued to cool through the Messinian (Pound et al., 2012a; Utescher et al., 2015; Herbert et al., 2016; Stein et al., 2016). Widespread alkenone data suggest that the Messinian included some of the largest cooling in sea surface temperatures of the Late Miocene, and a temperature minimum is recorded in the Arctic at around 6.5 Ma (Herbert et al., 2016; Stein et al., 2016). Despite this, the geographical distribution and percentages of CWS dinoflagellate cysts are similar to the Tortonian (Figures 4, 7). This may be an artefact of the current available data on global dinoflagellate cysts as much of the information comes from the North Atlantic, which by the Late Miocene was under the influence of the Gulf Stream current (Denk et al., 2013). The presence of CWS dinoflagellate cysts in the Late Miocene of offshore South Africa (Figure 4) has been used as an indicator for the presence of the cold Benguela Current (Hoetzel et al., 2017). The slightly reduced number of cold water dinoflagellate cysts in the Mediterranean during the Messinian, when compared to the Tortonian, is in agreement with alkenone data that shows warmer Messinian Sea Surface Temperatures (SSTs) than in the latest Tortonian (Tzarnova et al., 2015). The temporal resolution of the dataset does not allow any response to the Messinian Salinity Crisis to be detected (Flecker et al., 2015).

5.3.1 Spread of data in time and space

As previously mentioned, there are more records in the Northern Hemisphere than in the Southern Hemisphere. Due to this, the mean percentage of CWS for each stage (Figure 6a) was recalculated only using the records from the Northern Hemisphere (Figure 6b). The most obvious difference between the two methods (global versus northern only) was in the Tortonian. The mean percentage of CWS was higher for the Tortonian than for the immediately adjacent stages. This difference for the Tortonian can be explained by the Southern Hemisphere Tortonian having substantially more records than in the other intervals (Figures 4e, 5a), the majority of which have CWS values of 33% or higher. These records, between 65 and 70° S and 20 to 25° S, are numerous, with tightly constrained ages, and result in a much larger percentage of CWS in the Tortonian (19%, Figure 6a) than in the stages below and above (5% in the Serravallian and 12% in the Messinian). When only using data from the Northern Hemisphere, which has a more equal spatial distribution, there is a reduced discrepancy between the Tortonian and the immediately adjacent stages (Figure 6b). It is for this reason that the conclusions drawn from this study mainly concern the Northern Hemisphere. As the majority of data in the Northern Hemisphere were collected from the North Atlantic and Arctic oceans and the Mediterranean region, it is likely that the signal produced is from those areas, rather than for the whole of the Northern Hemisphere.

This implies that care must also be taken in the Northern Hemisphere where there are latitudinal bins represented which are devoid of data for every stage. For example, the three most northerly latitudinal bins only have data for the Pliocene, all of which have high percentages of CWS. To ensure that the Pliocene data were not skewing the results, further analysis of the data was carried out excluding latitudinal bins that did not have data for all stages (Figure 6b). Comparing results using all the Northern Hemisphere data, to those using simply latitudinal bins with data present for every stage (Figure 6b), indicates that the cooling was more extreme when all the data for the Northern Hemisphere were used. However, the overall trend is the same, and leads to the

conclusion that the absence of data in the high latitudes for stages other than the Pliocene has not skewed the results.

5.4 The Pliocene (5.33–2.59 Ma)

The Pliocene continued the trend of cooler climates with some relatively brief warm intervals (Haywood et al., 2013; 2016; Salzmann et al., 2013). Despite being cooler than the Miocene, the Pliocene was still significantly warmer than today (Haywood et al., 2013; Salzmann et al., 2013; Pound et al., 2015; Dowsett et al., 2016; Panitz et al., 2016). Compared to the Piacenzian, the modern dataset comprises records where all the species with known temperature preferences are CWS in the 30–35° N and 35–40° S latitudinal bins. By contrast, in the Piacenzian, the lowest latitudinal bin with a CWS percentage of 100% is 50–55° N and 65–70° S (Figures 4h, i). The Zanclean was warmer than the Piacenzian with a shallower Northern Hemisphere latitudinal gradient of CWS-dominated dinoflagellate cyst assemblages (Figure 7). The percentage of CWS increased most markedly in the high latitudes, from 45° N northwards (Figure 7e, f), thereby further steepening the latitudinal temperature gradient. Nikolaev et al. (1998) found that the latitudinal gradient increased by 4–5 °C during the Piacenzian, and Fedorov et al. (2013) demonstrated a 4–7 °C cooling of the mid to high latitudes of the North Atlantic and Pacific oceans. This cooling of the higher latitudes compared to the lower latitudes is a characteristic observed using a variety of proxies (Nikolaev et al., 1998; Brierley and Fedorov, 2010; Pound et al., 2012a; Fedorov et al., 2013; Herbert et al., 2016), and was associated with the development of ice in the high latitudes (Dolan et al., 2011; Dowsett et al., 2016).

Short-lived glaciations were infrequent in the Zanclean, but became more common in the Piacenzian as the global climate continued to cool (Lisiecki and Raymo, 2005; Miller et al., 2005; 2012). A generally warmer Zanclean, and a cooler Piacenzian, is consistent with the average percentage of CWS dinoflagellate cysts in the Zanclean (16%) and the Piacenzian (23%) (Figure 4), and is consistent with global alkenone records (Herbert et al., 2016). The East and West Antarctic ice sheets were

both well established by this time (Naish and Wilson, 2009; Dolan et al., 2011). Although the Southern Hemisphere lacks widespread dinoflagellate cyst records for the Piacenzian, the two data points proximal to the Antarctic Peninsula contain 100% CWS dinoflagellate cysts (Figure 4). Ice sheets in the Northern Hemisphere were significantly smaller, compared to the modern, or absent, which is consistent with WWS dinoflagellate cysts still being present in the high latitudes of the North Atlantic (Figure 4; Dolan et al., 2011; De Schepper et al., 2014; Panitz et al., 2016). Global climate started to significantly deteriorate (cooled) in the Piacenzian, leading to the intensification of the Northern Hemisphere glaciation around 2.75 Ma (Ravelo et al., 2004; Mudelsee and Raymo, 2005; De Schepper et al., 2014; Panitz et al., 2016).

The CAS continued to constrict during the Pliocene before finally closing around the Pliocene–Pleistocene boundary (Coates and Stallard, 2013; Osbourne et al., 2014). Neodymium isotopes show the exchange of waters until 2.5 Ma, but deep water exchanges had ceased by 7 Ma (Coates and Stallard, 2013; Osbourne et al., 2014). Interhemispheric foraminifera based Mg/Ca and $\delta^{18}\text{O}$ suggest that this continued constriction lead to greater heat transport in the Zanclean into the Northern Hemisphere, but reduced heat transport during the Piacenzian (Karas et al., 2017). These results are consistent with the latitudinal distribution of CWS dinoflagellate cysts in the Zanclean and Piacenzian (Figures 4, 7).

5.5 Driving factor of the cooling Neogene

The increase in CWS through the Neogene (Figures 6, 7) strongly supports the cooling trend seen in the benthic oxygen isotope stack, global vegetation records and global alkenone data (Zachos et al., 2008; Pound et al., 2012a; Salzmann et al., 2013; Utescher et al., 2015; Herbert et al., 2016).

Dinoflagellate cyst species that indicate cold waters are largely absent from the Aquitanian to the Serravallian (Figures 6, 7). This was followed, in the Late Miocene and Pliocene, by increasing proportions of CWS at individual data sites and the biogeographical expansion of cold water dinoflagellate cysts species towards the lower latitudes (Figures 4, 7). By the Piacenzian, a

forerunner of the modern latitudinal distribution of CWS was present (Figure 7). The global scale changes in dinoflagellate cysts through the Neogene points to a global scale control on Neogene climate. The most likely candidate would be changing concentrations of atmospheric CO₂ (Pound et al., 2011; 2012a; Bolton and Stoll, 2013). The role of CO₂ in driving Pliocene climate is well established (Haywood et al., 2016), whilst it has been strongly debated whether Miocene climate was also controlled by atmospheric CO₂ (Knorr et al., 2011; Pound et al., 2011; Bradshaw et al., 2012; Forrest et al., 2015). Much of the argument stems from older records of marine proxies for CO₂, which show flat-lining atmospheric CO₂ or values below the pre-industrial standard of 280 ppmv for most of the Miocene (Pagani et al., 1999; 2005; Beerling and Royer, 2011). The counterargument to these has been that these CO₂ records are incorrectly calculated (Ruddiman, 2010) or the true Miocene CO₂ level has yet to be detected in the record (Bolton and Stoll, 2013).

More recent records of Neogene CO₂ have demonstrated higher atmospheric values and high-resolution fluctuations that are in tune with other climate proxy records (Zhang et al., 2013; Greenop et al., 2014). Carbon dioxide as a controlling factor on Neogene climate is consistent with the global scale changes in CWS dinoflagellate cysts (Figures 4, 7). Modelling results compared to global datasets consistently show that higher (ca. 360-500 ppmv) CO₂ levels are necessary for successful simulation of Neogene climates (Dowsett et al., 2013; Bradshaw et al., 2015; Haywood et al., 2016; Stap et al., 2016). The global increases in Neogene cold water dinoflagellate cysts species are in agreement with the benthic $\delta^{18}\text{O}$ isotope stack (Zachos et al., 2008), global changes in biome distribution through the Neogene (Pound et al., 2012a; Salzmann et al., 2013), reconstructed marine and terrestrial temperatures (Utescher et al., 2015; Herbert et al., 2016), and the isotopic divergence of coccolithophores (Bolten et al., 2012; Bolten and Stoll, 2013). Such diverse and widespread evidence for a large-scale driver of global climate points to an overarching role of atmospheric CO₂.

6. Conclusions

Global datasets compiling previously published data are becoming more common and are increasingly used for evaluating environmental and climatic changes over longer time scales and over large regions (Salzmann et al., 2008; Masure and Vrielynck, 2009; Pound et al., 2012a; Masure et al., 2013; Woods et al., 2014). In our global compilation of Neogene dinoflagellate cyst data, we observed an increase in the mean percentage of CWS from the Early Miocene to Late Pliocene. An increase in the percentage of CWS, relative to the total number of species present with known temperature preferences, is qualitative evidence for decreasing SSTs. Our results agree very well with the gradual global climate cooling over the Neogene and increasing continental ice volume (Figure 6c; Zachos et al., 2001; 2008; Billups and Schrag, 2002; Ravelo et al., 2004; Shevenell et al., 2004; McKay et al., 2012; Miao et al., 2012; Pound et al., 2012a; Lear et al., 2015, Herbert et al., 2016). Our global compilation also allowed distinction between large scale climatic changes and local anomalies; for example, determining if the cooling trend had a global latitudinal and/or longitudinal gradient in the Miocene, Pliocene and modern surface ocean (subsections 5.1.1 to 5.1.5). From this study, the following conclusions can be drawn in relation to the research questions outlined in the introduction (section 1):

Can dinoflagellate cysts be used to determine global cooling in the Neogene?

- Dinoflagellate cysts are increasingly being used in palaeoclimate studies and this study corroborates their usefulness as a qualitative and relative temperature indicator over long timescales. Dinoflagellate cysts with known temperature preferences can be used to determine cooling on a global scale and the general cooling trend shown in this study broadly agrees with the global climate evolution in the Neogene (Figure 6c; Zachos et al., 2008). Our approach is validated by successful reconstructions of the modern sea surface temperature distribution on a global scale (Figure 4i, j).

Was the cooling during the Neogene uniform at all latitudes?

- Increases in the CWS percentage occurred most prominently in the mid to high latitudes, and less in the lower latitudes throughout the Neogene. This suggests that the mid to high latitudes underwent more cooling than the lower latitudes, at least in the Northern Hemisphere (Figure 7). The lower latitudinal temperature gradient during the Early and Mid Miocene, implied by smaller percentages of CWS in all latitudinal bins, agrees with terrestrial reconstructions from Pound et al. (2012a). These authors described a steepening of the latitudinal temperature gradient, as the high latitudes cooled more than the lower latitudes.

Was the rate of cooling uniform across the whole Neogene?

- Neogene climate cooling did not always occur at a steady rate and the most significant cooling occurred in the Pliocene, between the Zanclean and the Piacenzian (Figure 6a, b). There was a further decrease in temperature between the Piacenzian and the modern (Zonneveld et al., 2013b). The faster cooling rate from the Pliocene to the modern is consistent with the benthic $\delta^{18}\text{O}$ curve of Zachos et al. (2008).

Further progress in the global application of dinoflagellate cysts would be made with the collection of more primary data. In particular, targeting the Indian and Pacific oceans and the Southern Hemisphere, throughout the entire Neogene would substantially improve our knowledge of dinoflagellate biogeography. This would enable further comparison of temperature changes between the Northern and Southern Hemispheres, and permit analysis of the evolution of latitudinal temperature gradients. It would also be useful to obtain more data with a higher temporal resolution to analyse shorter events, such as the MMCO, rather than solely the long term trends. It is equally important to add further quantitative records to the TOPIS database to facilitate the detection of more refined temperature changes. However, this study unequivocally demonstrates that it is possible to use dinoflagellate cysts to determine large-scale climate changes through the Neogene.

Acknowledgments

This research was jointly funded by the British Geological Survey (BGS) University Funding Initiative (BUFI) and the University of Leeds. The BGS contract number is GA/12S/004, and the BUFI reference is S227. James B. Riding publishes with the approval of the Executive Director, British Geological Survey (NERC). Ruza F. Ivanovic is funded by a NERC Independent Research Fellowship (#NE/K008536/1). Stijn De Schepper is funded by the Norwegian Research Council (project 229819). Finally, we extend our sincere thanks to the journal editor and to two anonymous reviewers whose perceptive comments and critiques helped us to significantly improve the manuscript.

Figure captions

Supplementary data A: A list of the species with known temperature preferences used in this study and the references from which the information came.

Supplementary data B: A list of the localities used in this study and the publications from which the information came.

References

Abels, H., Hilgen, F., Krijgsman, W., Kruk, R., Raffi, I., Turco, E., Zachariasse, W., 2005. Long-period orbital control on middle Miocene global cooling: Integrated stratigraphy and astronomical tuning of the Blue Clay Formation on Malta. *Paleoceanography* 20, PA4012, doi: 10.1029/2004PA001129.

783 Badger, M.P., Lear, C.H., Pancost, R.D., Foster, G.L., Bailey, T.R., Leng, M.J., Abels, H.A., 2013. CO₂
784 drawdown following the middle Miocene expansion of the Antarctic Ice Sheet.
785 *Paleoceanography* 28, 42–53.

786 Balco, G., Rovey, C.W., 2010, Absolute chronology for major Pleistocene advances of the Laurentide
787 Ice Sheet: *Geology* 38, 795–798, DOI: 10.1130/G30946.1.

788 Banks, R., 1966. The cold layer in the Gulf of St. Lawrence. *Journal of Geophysical Research* 71,
789 1603–1610.

790 Beddow, H.M., Liebrand, D., Sluijs, A., Wade, B.S., Lourens, L.J., 2016. Global change across the
791 Oligocene-Miocene transition: High-resolution stable isotope records from IODP Site U1334
792 (equatorial Pacific Ocean). *Paleoceanography* 31, 81–97.

793 Beerling, D.J., Royer, D.L., 2011. Convergent cenozoic CO₂ history. *Nature Geoscience*, 4, 418–420.

794 Benson, R.B., Butler, R.J., Lindgren, J., Smith, A.S., 2009. Mesozoic marine tetrapod diversity: mass
795 extinctions and temporal heterogeneity in geological megabiases affecting vertebrates.
796 *Proceedings of the Royal Society of London* 277, 829–834.

797 Billups, K., Schrag, D., 2002. Paleotemperatures and ice volume of the past 27 Myr revisited with
798 paired Mg/Ca and 18O/16O measurements on benthic foraminifera. *Paleoceanography* 17,
799 1003–1014.

800 Bockelmann, F.D., Zonneveld, K.A., Schmidt, M., 2007. Assessing environmental control on
801 dinoflagellate cyst distribution in surface sediments of the Benguela upwelling region
802 (eastern South Atlantic). *Limnology and Oceanography*, 52, 2582–2594.

803 Bogus, K., Harding, I.C., King, A., Charles, A.J., Zonneveld, K.A., Versteegh, G.J., 2012. The
804 composition and diversity of dinosporin in species of the *Apectodinium* complex
805 (Dinoflagellata). *Review of Palaeobotany and Palynology* 183, 21–31.

806 Bogus, K., Mertens, K.N., Lauwaert, J., Harding, I.C., Vrielinck, H., Zonneveld, K.A., Versteegh, G.J.,
807 2014. Differences in the chemical composition of organic-walled dinoflagellate resting cysts
808 from phototrophic and heterotrophic dinoflagellates. *Journal of phycology* 50, 254–266.

809 Böhme, M., 2003. The Miocene climatic optimum: evidence from ectothermic vertebrates of Central
810 Europe. *Palaeogeography, Palaeoclimatology, Palaeoecology* 195, 389–401.

811 Bojar, A.-V., Hiden, H., Fenninger, A., Neubauer, F., 2004. Middle Miocene seasonal temperature
812 changes in the Styrian basin, Austria, as recorded by the isotopic composition of pectinid and
813 brachiopod shells. *Palaeogeography, Palaeoclimatology, Palaeoecology* 203, 95–105.

814 Bolton, C.T., Stoll, H.M., 2013. Late Miocene threshold response of marine algae to carbon dioxide
815 limitation. *Nature* 500, 558–562.

816 Bonnet, S., de Vernal, A., Gersonde, R., Lembke-Jene, L., 2012. Modern distribution of dinocysts from
817 the North Pacific Ocean (37–64 N, 144 E–148 W) in relation to hydrographic conditions, sea-
818 ice and productivity. *Marine Micropaleontology* 84, 87–113.

819 Bradshaw, C.D.C., Lunt, D.J., Flecker, R., Salzmann, U., Pound, M.J., Haywood, A.M., Eronen, J.T.,
820 2012. The relative roles of CO₂ and palaeogeography in determining Late Miocene climate:
821 results from a terrestrial model-data comparison. *Climate of the Past* 8, 1257–1285.

822 Bradshaw, C.D., Lunt, D.J., Flecker, R., Davies-Barnard, T., 2015. Disentangling the roles of late
823 Miocene palaeogeography and vegetation – Implications for climate sensitivity.
824 *Palaeogeography, Palaeoclimatology, Palaeoecology* 417, 17–34.

825 Brierley, C.M., Fedorov, A.V., 2010. Relative importance of meridional and zonal sea surface
826 temperature gradients for the onset of the ice ages and Pliocene-Pleistocene climate
827 evolution. *Paleoceanography* 25, doi: 10.1029/2009PA001809.

828 Brierley, C.M., Fedorov, A.V., 2016. Comparing the impacts of Miocene–Pliocene changes in inter-
829 ocean gateways on climate: Central American Seaway, Bering Strait, and Indonesia. *Earth
830 and Planetary Science Letters* 444, 116–130.

831 Brinkhuis, H., Bujak, J., Smit, J., Versteegh, G., Visscher, H., 1998. Dinoflagellate-based sea surface
832 temperature reconstructions across the Cretaceous–Tertiary boundary. *Palaeogeography,
833 Palaeoclimatology, Palaeoecology* 141, 67–83.

834 Bruch, A., Utescher, T., Mosbrugger, V., Gabrielyan, I., Ivanov, D., 2006. Late Miocene climate in the
835 circum-Alpine realm—a quantitative analysis of terrestrial palaeofloras. *Palaeogeography,*
836 *Palaeoclimatology, Palaeoecology* 238, 270–280.

837 Butler, R.J., Benson, R.B., Carrano, M.T., Mannion, P.D., Upchurch, P., 2011. Sea level, dinosaur
838 diversity and sampling biases: investigating the ‘common cause’ hypothesis in the terrestrial
839 realm. *Proceedings of the Royal Society of London B: Biological Sciences* 278, 1165–1170.

840 Coates, A.G., Stallard, R.F., 2013. How old is the Isthmus of Panama? *Bulletin of Marine Science* 89,
841 801–813.

842 Crame, J.A., 2001. Taxonomic diversity gradients through geological time. *Diversity and Distributions*
843 7, 175–189.

844 Crouch, E.M., Dickens, G.R., Brinkhuis, H., Aubry, M.-P., Hollis, C.J., Rogers, K.M., Visscher, H., 2003.
845 The *Apectodinium* acme and terrestrial discharge during the Paleocene–Eocene thermal
846 maximum: new palynological, geochemical and calcareous nannoplankton observations at
847 Tawanui, New Zealand. *Palaeogeography, Palaeoclimatology, Palaeoecology* 194, 387–403.

848 Crowley, T.J., 2000. Carbon dioxide and Phanerozoic climate. *Warm Climates in Earth History.*
849 Cambridge University Press Cambridge, 425–444.

850 Dale, B., 1983. Dinoflagellate resting cysts: “benthic plankton”. In: Fryxell, G.A. (editor). *Survival*
851 *strategies of the algae.* Cambridge University Press, 69–136.

852 Dale, B., 1996. Dinoflagellate cyst ecology: modeling and geological applications. In: Jansonius, J.,
853 McGregor, D.C. (editors). *Palynology: principles and applications.* American Association of
854 Stratigraphic Palynologists Foundation, Dallas 3, 1249–1275.

855 Denk, T., Grimm, G.W., Grímsson, F., Zetter, R., 2013. Evidence from "Köppen signatures" of fossil
856 plant assemblages for effective heat transport of Gulf Stream to subarctic North Atlantic
857 during Miocene cooling. *Biogeosciences* 10, 7927–7942.

858 De Schepper, S., Fischer, E.I., Groeneveld, J., Head, M.J., Matthiessen, J., 2011. Deciphering the
859 palaeoecology of Late Pliocene and Early Pleistocene dinoflagellate cysts. *Palaeogeography,*
860 *Palaeoclimatology, Palaeoecology* 309, 17–32.

861 De Schepper, S., Gibbard, P.L., Salzmann, U., Ehlers, J., 2014. A global synthesis of the marine and
862 terrestrial evidence for glaciation during the Pliocene Epoch. *Earth-Science Reviews* 135, 83–
863 102.

864 De Schepper, S., Head, M.J., Groeneveld, J., 2009. North Atlantic Current variability through marine
865 isotope stage M2 (circa 3.3 Ma) during the mid-Pliocene. *Paleoceanography* 24, doi:
866 4210.1029/2008pa001725.

867 De Schepper, S., Head, M.J., Louwye, S., 2004. New dinoflagellate cyst and *incertae sedis* taxa from
868 the Pliocene of northern Belgium, southern North Sea Basin. *Journal of Paleontology* 78,
869 625–644.

870 De Schepper, S., Schreck, M., Beck, K.M., Matthiessen, J., Fahl, K., Mangerud, G., 2015. Early Pliocene
871 onset of modern Nordic Seas circulation related to ocean gateway changes. *Nature*
872 *Communications* 6, doi: 10.1038/ncomms9659

873 De Vernal, A., Marret, F., 2007. Organic-walled dinoflagellate cysts: tracers of sea-surface conditions.
874 *Developments in Marine Geology* 1, 371–408, Elsevier B.V.

875 De Vernal, A., Rochon, A., Fréchette, B., Henry, M., Radi, T., Solignac, S., 2013. Reconstructing past
876 sea ice cover of the Northern Hemisphere from dinocyst assemblages: status of the
877 approach. *Quaternary Science Reviews* 79, 122–134.

878 De Verteuil, L., Norris, G., 1996. Miocene Dinoflagellate stratigraphy and systematics of Maryland
879 and Virginia. *Micropaleontology* 42, 1–82.

880 Diester-Haass, L., Meyers, P.A., Rothe, P., 1990. Miocene history of the Benguela Current and
881 Antarctic ice volumes: Evidence from rhythmic sedimentation and current growth across the
882 Walvis Ridge (Deep Sea Drilling Project Sites 362 and 532). *Paleoceanography* 5, 685–707.

883 Dolan, A.M., Haywood, A.M., Hill, D.J., Dowsett, H.J., Hunter, S.J., Lunt, D.J., Pickering, S.J., 2011.
884 Sensitivity of Pliocene ice sheets to orbital forcing. *Palaeogeography, Palaeoclimatology,*
885 *Palaeoecology* 309, 98–110.

886 Donders, T., Weijers, J., Munsterman, D., Kloosterboer-Van Hoeve, M., Buckles, L., Pancost, R.,
887 Schouten, S., Damsté, J. S., Brinkhuis, H., 2009. Strong climate coupling of terrestrial and
888 marine environments in the Miocene of northwest Europe. *Earth and Planetary Science*
889 *Letters* 281, 215–225.

890 Dowsett, H., Dolan, A., Rowley, D., Moucha, R., Forte, A.M., Mitrovica, J.X., Pound, M., Salzmann, U.,
891 Robinson, M., Chandler, M., Foley, K., Haywood, A., 2016. The PRISM4 (mid-Piacenzian)
892 paleoenvironmental reconstruction. *Climate of the Past* 12, 1519–1538.

893 Dowsett, H.J., Foley, K.M., Stoll, D.K., Chandler, M.A., Sohl, L.E., Bentsen, M., Otto-Bliesner, B.L.,
894 Bragg, F.J., Chan, W.-L., Contoux, C., Dolan, A.M., Haywood, A.M., Jonas, J.A., Jost, A.,
895 Kamae, Y., Lohmann, G., Lunt, D.J., Nisancioglu, K.H., Abe-Ouchi, A., Ramstein, G.,
896 Riesselman, C.R., Robinson, M.M., Rosenbloom, N.A., Salzmann, U., Stepanek, C., Strother,
897 S.L., Ueda, H., Yan, Q., Zhang, Z., 2013. Sea Surface Temperature of the mid-Piacenzian
898 Ocean: A Data-Model Comparison. *Science Reports* 3.

899 Fauquette, S., Suc, J.-P., Jiménez-Moreno, G., Micheels, A., Jost, A., Favre, E., Bachiri-Taoufiq, N.,
900 Bertini, A., Clet-Pellerin, M., Diniz, F., 2007. Latitudinal climatic gradients in the Western
901 European and Mediterranean regions from the Mid-Miocene (c. 15 Ma) to the Mid-Pliocene
902 (c. 3.5 Ma) as quantified from pollen data. In: Williams, M., Haywood, A.M., Gregory, F.J.,
903 Schmidt, D.N., (editors). *Deep-time perspectives on climate change. The*
904 *Micropalaeontological Society Special Publications. The Geological Society, London*, 481–
905 502.

906 Fauquette, S., Bernet, M., Suc, J.-P., Grosjean, A.-S., Guillot, S., van der Beek, P., Jourdan, S., Popescu,
907 S.-M., Jiménez-Moreno, G., Bertini, A., Pittet, B., Tricart, P., Dumont, T., Schwartz, S., Zheng,

908 Z., Roche, E., Pavia, G., Gardien, V., 2015. Quantifying the Eocene to Pleistocene topographic
 909 evolution of the southwestern Alps, France and Italy. *Earth and Planetary Science Letters*
 910 412, 220-234.

911 Fedorov, A.V., Brierley, C.M., Lawrence, K.T., Liu, Z., Dekens, P.S., Ravelo, A.C., 2013. Patterns and
 912 mechanisms of early Pliocene warmth. *Nature* 496, 43–49.

913 Fensome, R.A., MacRae, R.A., Williams, G.L., 2008. DINOFLAJ2, version 1. American Association of
 914 Stratigraphic Palynologists, Data Series, 1, 937p.

915 Fensome, R.A., Taylor, F.J.R., Norris, G., Sarjeant, W.A.S., Wharton, D.I., Williams, G.L., 1993. A
 916 classification of living and fossil dinoflagellates. American Museum of Natural History,
 917 Micropaleontology Special Publication 7. Sheridan Press, Hanover, PA. 351 p.

918 Flecker, R., Krijgsman, W., Capella, W., De Castro Martíns, C., Dmitrieva, E., Mayser, J.P., Marzocchi,
 919 A., Modestu, S., Ochoa, D., Simon, D., 2015. Evolution of the Late Miocene Mediterranean–
 920 Atlantic gateways and their impact on regional and global environmental change. *Earth-
 921 Science Reviews* 150, 365–392.

922 Flower, B., Kennett, J., 1993. Middle Miocene ocean-climate transition: High-resolution oxygen and
 923 carbon isotopic records from Deep Sea Drilling Project Site 588A, southwest Pacific.
 924 *Paleoceanography* 8, 811–843.

925 Flower, B.P., Kennett, J.P., 1994. The middle Miocene climatic transition: East Antarctic ice sheet
 926 development, deep ocean circulation and global carbon cycling. *Palaeogeography,
 927 Palaeoclimatology, Palaeoecology* 108, 537–555.

928 Forrest, M., Eronen, J.T., Utescher, T., Knorr, G., Stepanek, C., Lohmann, G., Hickler, T., 2015.
 929 Climate-vegetation modelling and fossil plant data suggest low atmospheric CO₂ in the late
 930 Miocene. *Climate of the Past* 11, 1701–1732.

931 Foster, G.L., Lear, C.H., Rae, J.W., 2012. The evolution of pCO₂, ice volume and climate during the
 932 middle Miocene. *Earth and Planetary Science Letters* 341, 243–254.

933 Gibbard, P.L., Head, M.J., Walker, M.J.C., 2010. Formal ratification of the Quaternary System/Period
934 and the Pleistocene Series/Epoch with a base at, 2.58 Ma. *Journal of Quaternary Science* 25,
935 96–102.

936 Gradstein, F.M., Ogg, G., Schmitz, M., 2012. *The Geologic Time Scale 2012*, Amsterdam, Elsevier, 2-
937 Volume Set, 1144 p.

938 Graham, A., 2009. The Andes: A geological overview from a biological perspective. *Annals of the*
939 *Missouri Botanical Garden* 96, 371-385.

940 Greenop, R., Foster, G.L., Wilson, P.A., Lear, C.H., 2014. Middle Miocene climate instability
941 associated with high-amplitude CO₂ variability. *Paleoceanography* 29, 845-853.

942 Grunert, P., Tzanova, A., Harzhauser, M., Piller, W.E., 2014. Mid-Burdigalian Paratethyan alkenone
943 record reveals link between orbital forcing, Antarctic ice-sheet dynamics and European
944 climate at the verge to Miocene Climate Optimum. *Global and Planetary Change* 123, 36–43.

945 Hansen, J., Sato, M., Russell, G., Kharecha, P., 2013. Climate sensitivity, sea level and atmospheric
946 carbon dioxide. *Philosophical Transactions of the Royal Society of London A: Mathematical,*
947 *Physical and Engineering Sciences* 371, doi: 10.1098/rsta.2012.0294.

948 Harland, R., 1983. Distribution maps of recent dinoflagellate cysts in bottom sediments from the
949 North-Atlantic Ocean and adjacent seas. *Palaeontology* 26, 321–387.

950 Harland, R., Pudsey, C.J., 1999. Dinoflagellate cysts from sediment traps deployed in the
951 Bellingshausen, Weddell and Scotia seas, Antarctica. *Marine Micropaleontology*, 37, 77–99.

952 Haywood, A., Hill, D., Dolan, A., Otto-Bliesner, B., Bragg, F., Chan, W.-L., Chandler, M., Contoux, C.,
953 Dowsett, H., Jost, A., 2013. Large-scale features of Pliocene climate: results from the
954 Pliocene Model Intercomparison Project. *Climate of the Past* 9, 191–209.

955 Haywood, A.M., Dowsett, H.J., Dolan, A.M., Rowley, D., Abe-Ouchi, A., Otto-Bliesner, B., Chandler,
956 M.A., Hunter, S.J., Lunt, D.J., Pound, M., Salzmann, U., 2016. The Pliocene Model

957 Intercomparison Project (PlioMIP) Phase 2: scientific objectives and experimental design.
 958 Climate of the Past 12, 663–675.

959 Haywood, A.M., Valdes, P.J., Sellwood, B.W., 2002. Magnitude of climate variability during middle
 960 Pliocene warmth: a palaeoclimate modelling study. *Palaeogeography, Palaeoclimatology,*
 961 *Palaeoecology* 188, 1–24.

962 Head, M.J., Norris, G., Mudie, P.J., 1989. New species of dinocysts and a new species of acritarch
 963 from the upper Miocene and lowermost Pliocene, ODP Leg 105, Site 646, Labrador Sea.
 964 *Proceedings of the Ocean Drilling Program* 105, 453–466.

965 Head, M.J., 1994. Morphology and paleoenvironmental significance of the Cenozoic dinoflagellate
 966 genera *Tectatodinium* and *Habibacysta*. *Micropaleontology* 40, 289–321.

967 Head, M.J., 1997. Thermophilic dinoflagellate assemblages from the mid Pliocene of eastern
 968 England. *Journal of Paleontology* 71, 165–193.

969 Heinrich, S., Zonneveld, K.A., Bickert, T., Willems, H., 2011. The Benguela upwelling related to the
 970 Miocene cooling events and the development of the Antarctic Circumpolar Current:
 971 Evidence from calcareous dinoflagellate cysts. *Paleoceanography* 26, doi:
 972 10.1029/2010PA002065.

973 Hennissen, J.A., Head, M.J., De Schepper, S., Groeneveld, J., 2014. Palynological evidence for a
 974 southward shift of the North Atlantic Current at ~ 2.6 Ma during the intensification of late
 975 Cenozoic Northern Hemisphere glaciation. *Paleoceanography* 29, 564–580.

976 Hennissen, J.A., Head, M.J., De Schepper, S. and Groeneveld, J., 2017. Dinoflagellate cyst
 977 paleoecology during the Pliocene–Pleistocene climatic transition in the North Atlantic.
 978 *Palaeogeography, Palaeoclimatology, Palaeoecology* 470, 81–108.

979 Herbert, T.D., Lawrence, K.T., Tzanova, A., Peterson, L.C., Caballero-Gill, R., Kelly, C.S., 2016, Late
 980 Miocene global cooling and the rise of modern ecosystems: *Nature Geoscience* doi:
 981 10.1038/ngeo2813.

982 Hoetzel, S., Dupont, L.M., Wefer, G., 2015. Miocene–Pliocene vegetation change in south-western
983 Africa (ODP Site 1081, offshore Namibia). *Palaeogeography, Palaeoclimatology,*
984 *Palaeoecology* 423, 102–108.

985 Hopkins, J.A., McCarthy, F.M.G., 2002. Post-depositional palynomorph degradation in Quaternary
986 shelf sediments: A laboratory experiment studying the effects of progressive oxidation.
987 *Palynology* 26, 167–184.

988 Hunter, S.J., Haywood, A.M., Valdes, P.J., Francis, J.E., Pound, M.J., 2013. Modelling equable climates
989 of the Late Cretaceous: Can new boundary conditions resolve data–model discrepancies?
990 *Palaeogeography, Palaeoclimatology, Palaeoecology* 392, 41–51.

991 Jablonski, D., Roy, K., Valentine, J.W., Price, R.M., Anderson, P.S., 2003. The impact of the pull of the
992 recent on the history of marine diversity. *Science* 300, 1133–1135.

993 Jansen, E., Bleil, U., Henrich, R., Kringstad, L., Slettemark, B., 1988, Paleoenvironmental changes in
994 the Norwegian Sea and the northeast Atlantic during the last 2.8 Ma: Deep Sea Drilling
995 Project/Ocean Drilling Program sites 610, 642, 643 and 644: *Paleoceanography* 3, 563–581.

996 Karas, C., Nürnberg, D., Bahr, A., Groeneveld, J., Herrle, J.O., Tiedemann, R., 2017. Pliocene oceanic
997 seaways and global climate. *Scientific Reports* 7, 39842.

998 Kawamura, H., 2004. Dinoflagellate cyst distribution along a shelf to slope transect of an oligotrophic
999 tropical sea (Sunda Shelf, South China Sea). *Phycological Research* 52, 355–375.

1000 Knorr, G., Butzin, M., Micheels, A., Lohmann, G., 2011. A warm Miocene climate at low atmospheric
1001 CO₂ levels. *Geophysical Research Letters* 38, doi: 10.1029/2011GL048873.

1002 Knorr, G., Lohmann, G., 2014. Climate warming during Antarctic ice sheet expansion at the Middle
1003 Miocene transition. *Nature Geoscience* 7, 376–381.

1004 Kroh, A., 2007. Climate changes in the Early to Middle Miocene of the Central Paratethys and the
1005 origin of its echinoderm fauna. *Palaeogeography, Palaeoclimatology, Palaeoecology* 253,
1006 169–207.

1007 Kürschner, W.M., Kvaček, Z., Dilcher, D.L., 2008. The impact of Miocene atmospheric carbon dioxide
 1008 fluctuations on climate and the evolution of terrestrial ecosystems. *Proceedings of the*
 1009 *National Academy of Sciences* 105, 449–453.

1010 Lear, C.H., Coxall, H.K., Foster, G.L., Lunt, D.J., Mawbey, E.M., Rosenthal, Y., Sosdian, S.M., Thomas,
 1011 E., Wilson, P.A., 2015. Neogene ice volume and ocean temperatures: Insights from infaunal
 1012 foraminiferal Mg/Ca paleothermometry. *Paleoceanography* 30, 1437–1454.

1013 Limoges, A., Londeix, L., de Vernal, A., 2013. Organic-walled dinoflagellate cyst distribution in the
 1014 Gulf of Mexico. *Marine Micropaleontology* 102, 51–68.

1015 Lisiecki, L.E., Raymo, M.E., 2005. A Pliocene-Pleistocene stack of 57 globally distributed benthic $\delta^{18}\text{O}$
 1016 records. *Paleoceanography* 20, doi: 10.1029/2004PA001071.

1017 Long, Z., Perrie, W., Chassé, J., Brickman, D., Guo, L., Drozdowski, A., Hu, H., 2015. Impacts of climate
 1018 change in the Gulf of St. Lawrence. *Atmosphere-Ocean* 54, 1–15.

1019 Londeix, L., Jan du Chêne, R., 1998. Burdigalian dinocyst stratigraphy of the stratotypic area
 1020 (Bordeaux, France). *Geobios* 31, 283–294.

1021 Louwye, S., De Coninck, J., Verniers, J., 2000. Shallow marine Lower and Middle Miocene deposits at
 1022 the southern margin of the North Sea Basin (northern Belgium): dinoflagellate cyst
 1023 biostratigraphy and depositional history. *Geological Magazine* 137, 381–394.

1024 Louwye, S., De Schepper, S., Laga, P., Vandenberghe, N., 2007. The upper Miocene of the southern
 1025 North Sea Basin (northern Belgium): a palaeoenvironmental and stratigraphical
 1026 reconstruction using dinoflagellate cysts. *Geological Magazine* 144, 33–52.

1027 Louwye, S., De Schepper, S., 2010. The Miocene–Pliocene hiatus in the southern North Sea Basin
 1028 (northern Belgium) revealed by dinoflagellate cysts. *Geological Magazine* 147, 760–776.

1029 Mannion, P.D., Upchurch, P., Benson, R.B., Goswami, A., 2014. The latitudinal biodiversity gradient
 1030 through deep time. *Trends in Ecology and Evolution* 29, 42–50.

- 1031 Markwick, P.J., Rowley, D.B., Ziegler, A.M., Hulver, M.L., Valdes, P.J., Sellwood, B.W., 2000. Late
1032 Cretaceous and Cenozoic global palaeogeographies: Mapping the transition from a “hot-
1033 house” to an “ice-house” world. *Geologiska i Stockholm Gorehandlingar* 122, 103 p.
- 1034 Marret, F., 1993. Les effets de l'acétolyse sur les assemblages des kystes de dinoflagellés.
1035 *Palynosciences* 2, 267–272.
- 1036 Marret, F., Zonneveld, K.A., 2003. Atlas of modern organic-walled dinoflagellate cyst distribution.
1037 *Review of Palaeobotany and Palynology* 125, 1–200.
- 1038 Masure, E., Aumar, A.-M., Vrielynck, B., 2013. Worldwide palaeogeography of Aptian and Late Albian
1039 dinoflagellate cysts: Implications for sea-surface temperature gradients and palaeoclimate.
1040 In: Lewis, J.M., Marret, F., Bradley, L., (editors). *Biological and Geological Perspectives of*
1041 *Dinoflagellates*. The Micropalaeontological Society, Special Publications. Geological Society,
1042 London, 97–125.
- 1043 Masure, E., Vrielynck, B., 2009. Late Albian dinoflagellate cyst paleobiogeography as indicator of
1044 asymmetric sea surface temperature gradient on both hemispheres with southern high
1045 latitudes warmer than northern ones. *Marine Micropaleontology* 70, 120–133.
- 1046 McCarthy, F.M., Mudie, P.J., 1996. Palynology and dinoflagellate biostratigraphy of upper Cenozoic
1047 sediments from Sites 898 and 900, Iberia Abyssal Plain. *Proceedings of the Ocean Drilling*
1048 *Program, Scientific Results* 149, 241–265.
- 1049 McKay, R., Naish, T., Carter, L., Riesselman, C., Dunbar, R., Sjunneskog, C., Winter, D., Sangiorgi, F.,
1050 Warren, C., Pagani, M., 2012. Antarctic and Southern Ocean influences on Late Pliocene
1051 global cooling. *Proceedings of the National Academy of Sciences* 109, 6423–6428.
- 1052 Mertens, K.N., Takano, Y., Head, M.J., Matsuoka, K., 2014. Living fossils in the Indo-Pacific warm
1053 pool: A refuge for thermophilic dinoflagellates during glaciations. *Geology* 42, 531–534.
- 1054 Mertens, K.N., Verhoeven, K., Verleye, T., Louwye, S., Amorim, A., Ribeiro, S., Deaf, A.S., Harding,
1055 I.C., de Schepper, S., González, C., Kodrans-Nsiah, M., de Vernal, A., Henry, M., Radi, T.,
1056 Dybkjær, K., Poulsen, N.E., Feist-Burkhardt, S., Chitolie, J., Heilmann-Clausen, C., Londeix, L.,

1057 Turon, J.-L., Marret, F., Matthiessen, J., McCarthy, F.M.G., Prasad, V., Pospelova, V., Kyffin
 1058 Hughes, J.E., Riding, J.B., Rochon, A., Sangiorgi, F., Welters, N., Sinclair, N., Thun, C., Soliman,
 1059 A., van Nieuwenhove, N., Vink, A., Young, M., 2009. Determining the absolute abundance of
 1060 dinoflagellate cysts in recent marine sediments: The *Lycopodium* marker-grain method put
 1061 to the test. *Review of Palaeobotany and Palynology* 157, 238–252.

1062 Miao, Y., Herrmann, M., Wu, F., Yan, X., Yang, S., 2012. What controlled Mid–Late Miocene long-
 1063 term aridification in Central Asia?—Global cooling or Tibetan Plateau uplift: A review. *Earth-
 1064 Science Reviews* 112, 155–172.

1065 Miller, K.G., Kominz, M.A., Browning, J.V., Wright, J.D., Mountain, G.S., Katz, M.E., Sugarman, P.J.,
 1066 Cramer, B.S., Christie-Blick, N., Pekar, S.F., 2005. The Phanerozoic record of global sea-level
 1067 change. *Science* 310, 1293–1298.

1068 Miller, K.G., Wright, J.D., Browning, J.V., Kulpecz, A., Kominz, M., Naish, T.R., Cramer, B.S., Rosenthal,
 1069 Y., Peltier, W.R., Sossian, S., 2012. High tide of the warm Pliocene: Implications of global sea
 1070 level for Antarctic deglaciation. *Geology* 40, 407–410.

1071 Mittelbach, G.G., Schemske, D.W., Cornell, H.V., Allen, A.P., Brown, J.M., Bush, M.B., Harrison, S.P.,
 1072 Hurlbert, A.H., Knowlton, N., Lessios, H.A., 2007. Evolution and the latitudinal diversity
 1073 gradient: speciation, extinction and biogeography. *Ecology Letters* 10, 315–331.

1074 Montes, C., Cardona, A., Jaramillo, C., Pardo, A., Silva, J.C., Valencia, V., Ayala, C., Pérez-Angel, L.C.,
 1075 Rodríguez-Parra, L.A., Ramírez, V., Niño, H., 2015. Middle Miocene closure of the Central
 1076 American Seaway. *Science* 348, 226–229.

1077 Moran, K., Backman, J., Brinkhuis, H., Clemens, S.C., Cronin, T., Dickens, G.R., Eynaud, F., Gattacceca,
 1078 J., Jakobsson, M., Jordan, R.W., Kaminski, M., King, J., Koc, N., Krylov, A., Martinez, N.,
 1079 Matthiessen, J., McInroy, D., Moore, T.C., Onodera, J., O'Regan, M., Pälike, H., Rea, B., Rio,
 1080 D., Sakamoto, T., Smith, D.C., Stein, R., St John, K., Suto, I., Suzuki, N., Takahashi, K.,
 1081 Watanabe, M., Yamamoto, M., Farrell, J., Frank, M., Kubik, P., Jokat, W., Kristoffersen, Y.,
 1082 2006. The Cenozoic palaeoenvironment of the Arctic Ocean. *Nature* 441, 601–605.

1083 Mudelsee, M., Raymo, M.E., 2005. Slow dynamics of the Northern Hemisphere glaciation.
 1084 Paleoceanography 20, doi: 10.1029/2005PA001153.

1085 Mudie, P.J., McCarthy, F.M., 2006. Marine palynology: potentials for onshore—offshore correlation
 1086 of Pleistocene-Holocene records. Transactions of the Royal Society of South Africa 61, 139–
 1087 157.

1088 Naish, T.R., Wilson, G.S., 2009. Constraints on the amplitude of Mid-Pliocene (3.6–2.4 Ma) eustatic
 1089 sea-level fluctuations from the New Zealand shallow-marine sediment record. Philosophical
 1090 Transactions of the Royal Society of London A: Mathematical, Physical and Engineering
 1091 Sciences 367, 169–187.

1092 NASA Ocean Biology (OB.DAAC), 2014. Mean annual sea surface temperature for
 1093 the period 2009–2013 (composite dataset created by UNEP-WCMC). Data obtained
 1094 from the Moderate Resolution Imaging Spectroradiometer (MODIS) Aqua Ocean
 1095 Colour website (NASA OB.DAAC, Greenbelt, MD, USA). Accessed 28/11/2014. URL:
 1096 <http://oceancolor.gsfc.nasa.gov/cgi/l3>. Cambridge (UK): UNEP World Conservation
 1097 Monitoring Centre. URL: <http://data.unep-wcmc.org/datasets/36>.

1098 Nikolaev, S., Oskina, N., Blyum, N., Bubenshchikova, N., 1998. Neogene–Quaternary variations of the
 1099 Pole–Equator temperature gradient of the surface oceanic waters in the North Atlantic and
 1100 North Pacific. Global and Planetary Change 18, 85–111.

1101 Osbourne, A.H., Newkirk, D.R., Groeneveld, J., Martin, E.E., Tiedemann, R., Frank, M., 2014. The
 1102 seawater neodymium and lead isotope record of the final stages of Central American Seaway
 1103 closure. Paleoceanography 29, pp.715–729.

1104 Pagani, M., Arthur, M.A., Freeman, K.H., 1999. Miocene evolution of atmospheric carbon dioxide.
 1105 Paleoceanography 14, 273–292.

1106 Pagani, M., Zachos, J.C., Freeman, K.H., Tipler, B., Bohaty, S., 2005. Marked decline in atmospheric
 1107 carbon dioxide concentrations during the Paleogene. Science 309, 600–603.

1108 Panitz, S., Salzmann, U., Risebrobakken, B., De Schepper, S., Pound, M.J., 2016. Climate variability
1109 and long-term expansion of peat lands in Arctic Norway during the late Pliocene (ODP Site
1110 642, Norwegian Sea). *Climate of the Past Discussions* 11, 5755–5798.

1111 Pearson, P.N., Palmer, M.R., 2000. Atmospheric carbon dioxide concentrations over the past 60
1112 million years. *Nature* 406, 695–699.

1113 Pospelova, V., de Vernal, A., Pedersen, T.F., 2008. Distribution of dinoflagellate cysts in surface
1114 sediments from the northeastern Pacific Ocean (43–25 N) in relation to sea-surface
1115 temperature, salinity, productivity and coastal upwelling. *Marine Micropaleontology* 68, 21–
1116 48.

1117 Potter, P.E., Szatmari, P., 2009. Global Miocene tectonics and the modern world. *Earth–Science*
1118 *Reviews* 96, 279–295.

1119 Pound, M.J., Haywood, A.M., Salzmann, U., Riding, J.B., Lunt, D.J., Hunter, S.J., 2011. A Tortonian
1120 (Late Miocene, 11.61–7.25 Ma) global vegetation reconstruction. *Palaeogeography,*
1121 *Palaeoclimatology, Palaeoecology* 300, 29–45.

1122 Pound, M.J., Haywood, A.M., Salzmann, U., Riding, J.B., 2012a. Global vegetation dynamics and
1123 latitudinal temperature gradients during the Mid to Late Miocene (15.97–5.33 Ma). *Earth-*
1124 *Science Reviews* 112, 1–22.

1125 Pound, M.J., Riding, J.B., Donders, T.H., Daskova, J., 2012b. The palynostratigraphy of the
1126 Brassington Formation (Upper Miocene) of the southern Pennines, central England.
1127 *Palynology* 36, 26–37.

1128 Pound, M.J., Lowther, R.I., Peakall, J., Chapman, R.J., Salzmann, U., 2015. Palynological evidence for a
1129 warmer boreal climate in the Late Pliocene of the Yukon Territory, Canada. *Palynology* 39,
1130 91–102.

1131 Pound, M.J., Riding, J.B., 2016. Palaeoenvironment, palaeoclimate and age of the Brassington
1132 Formation (Miocene) of Derbyshire, UK. *Journal of the Geological Society* 173, 306–319.

1133 Pound, M.J., Salzmann, U., 2017. Heterogeneity in global vegetation and terrestrial climate change
 1134 during the late Eocene to early Oligocene transition. *Scientific Reports* 7, 43386.

1135 Prebble, J.G., Reichgelt, T., Mildenhall, D.C., Greenwood, D.R., Raine, J.I., Kennedy, E.M., Seebeck,
 1136 H.C., 2017. Terrestrial climate evolution in the Southwest Pacific over the past 30 million
 1137 years. *Earth and Planetary Science Letters* 459, 136–144.

1138 Pudsey, C.J., Harland, R., 2001. Data Report: Dinoflagellate cyst analysis of Neogene sediments from
 1139 Sites 1095 and 1096, Antarctic Peninsula Continental Rise. *Proceedings of the Ocean Drilling*
 1140 *Program* 178, 1–10.

1141 Quaijtaal, W., Donders, T.H., Persico, D., Louwye, S., 2014. Characterising the middle Miocene Mi-
 1142 events in the Eastern North Atlantic realm: A first high-resolution marine palynological
 1143 record from the Porcupine Basin. *Palaeogeography, Palaeoclimatology, Palaeoecology* 399,
 1144 140–159.

1145 Radi, T., De Vernal, A., 2008. Dinocysts as proxy of primary productivity in mid–high latitudes of the
 1146 Northern Hemisphere. *Marine Micropaleontology* 68, 84–114.

1147 Raup, D.M., 1979. Biases in the fossil record of species and genera. *Bulletin of the Carnegie Museum*
 1148 *of Natural History* 13, 85–91.

1149 Ravelo, A.C., Andreasen, D.H., Lyle, M., Lyle, A.O., Wara, M.W., 2004. Regional climate shifts caused
 1150 by gradual global cooling in the Pliocene epoch. *Nature* 429, 263–267.

1151 Raymo, M., Ruddiman, W.F., 1992. Tectonic forcing of late Cenozoic climate. *Nature* 359, 117–122.

1152 Raymo, M.E., Ruddiman, W.F., Froelich, P.N., 1988. Influence of late Cenozoic mountain building on
 1153 ocean geochemical cycles. *Geology* 16, 649–653.

1154 Richerol, T., Pienitz, R., Rochon, A., 2012. Modern dinoflagellate cyst assemblages in surface
 1155 sediments of Nunatsiavut fjords (Labrador, Canada). *Marine Micropaleontology* 88, 54–64.

1156 Riding, J.B., Kyffin-Hughes, J.E., 2004. A review of the laboratory preparation of palynomorphs with a
 1157 description of an effective non-acid technique. *Revista Brasileira de Paleontologia* 7, 13–44.

1158 Riding, J.B., Pound, M.J., Hill, T.C.B., Stukins, S., Feist-Burkhardt, S., 2012. The John Williams Index of
1159 Palaeopalynology. *Palynology* 36, 224–233.

1160 Robert, C., Diester-Haass, L., Paturel, J., 2005. Clay mineral assemblages, siliciclastic input and
1161 paleoproductivity at ODP Site 1085 off Southwest Africa: a late Miocene–early Pliocene
1162 history of Orange river discharges and Benguela current activity, and their relation to global
1163 sea level change. *Marine Geology* 216, 221–238.

1164 Robinson, M.M., Valdes, P.J., Haywood, A.M., Dowsett, H.J., Hill, D.J., Jones, S.M., 2011. Bathymetric
1165 controls on Pliocene North Atlantic and Arctic sea surface temperature and deepwater
1166 production. *Palaeogeography, Palaeoclimatology, Palaeoecology* 309, 92–97.

1167 Rochon, A., Vernal, A.D., Turon, J.-L., Matthiessen, J., Head, M.J., 1999. Distribution of recent
1168 dinoflagellate cysts in surface sediments from the North Atlantic Ocean and adjacent seas in
1169 relation to sea-surface parameters. *American Association of Stratigraphic Palynologists*
1170 *Contribution Series* 35, 146 p.

1171 Ruddiman, W.F., 2010. A paleoclimatic enigma? *Science* 328, 838–839.

1172 Ruddiman, W.F., 2013. *Tectonic uplift and climate change*, Springer Science and Business Media 534
1173 p.

1174 Salzmann, U., Haywood, A., Lunt, D., Valdes, P., Hill, D., 2008. A new global biome reconstruction and
1175 data-model comparison for the middle Pliocene. *Global Ecology and Biogeography* 17, 432–
1176 447.

1177 Salzmann, U., Dolan, A.M., Haywood, A.M., Chan, W.-L., Voss, J., Hill, D.J., Abe-Ouchi, A., Otto-
1178 Bliesner, B., Bragg, F.J., Chandler, M.A., Contoux, C., Dowsett, H.J., Jost, A., Kamae, Y.,
1179 Lohmann, G., Lunt, D.J., Pickering, S.J., Pound, M.J., Ramstein, G., Rosenbloom, N.A., Sohl, L.,
1180 Stepanek, C., Ueda, H., Zhang, Z., 2013. Challenges in quantifying Pliocene terrestrial
1181 warming revealed by data-model discord. *Nature Climate Change* 3, 969–974.

1182 Saucier, F.J., Roy, F., Gilbert, D., Pellerin, P., Ritchie, H., 2003. Modeling the formation and circulation
1183 processes of water masses and sea ice in the Gulf of St. Lawrence, Canada. *Journal of*
1184 *Geophysical Research: Oceans* 108, doi: 10.1029/2000JC000686.

1185 Savin, S.M., Douglas, R.G., Stehli, F.G., 1975. Tertiary marine paleotemperatures. *Geological Society*
1186 *of America Bulletin* 86, 1499–1510.

1187 Schreck, M., Matthiessen, J., 2013. *Batiacasphaera micropapillata*: Palaeobiogeographic distribution
1188 and palaeoecological implications of a critical Neogene species complex. In: Lewis, J.M.,
1189 Marret, F., Bradley, L., (editors). *Biological and Geological Perspectives of Dinoflagellates*.
1190 *The Micropalaeontological Society, Special Publications*. Geological Society, London, 301–
1191 314.

1192 Schreck, M., Meheust, M., Stein, R., Matthiessen, J., 2013. Response of marine palynomorphs to
1193 Neogene climate cooling in the Iceland Sea (ODP Hole 907A). *Marine Micropaleontology*
1194 101, 49–67.

1195 Shackleton, N.J., Backman, J., Zimmerman, H., Kent, D.V., Hall, M.A., Roberts, D.G., Schnitker, D.,
1196 Baldauf, J.G., Desprairies, A., Homrighausen, R., Huddleston, P., Keene, J.B., Kaltenback, A.J.,
1197 Krumsiek, K.A.O., et al., 1984, Oxygen Isotope Calibration of the Onset of Ice-Rafting and
1198 History of Glaciation in the North-Atlantic Region: *Nature* 307, 620–623.

1199 Shackleton, N.J., Kennett, J., 1975. Paleotemperature history of the Cenozoic and initiation of
1200 Antarctic glaciation: Oxygen and carbon isotope analyses in DSDP sites 277 279, and 281.
1201 *Initial Reports of the Deep Sea Drilling Project* 29, 743–755.

1202 Shevenell, A.E., Kennett, J.P., Lea, D.W., 2004. Middle Miocene southern ocean cooling and Antarctic
1203 cryosphere expansion. *Science* 305, 1766–1770.

1204 Siesser, W.G., 1980. Late Miocene origin of the Benguela upswelling system off northern Namibia.
1205 *Science* 208, 283–285.

1206 Sijp, W.P., Anna, S., Dijkstra, H.A., Flögel, S., Douglas, P.M., Bijl, P.K., 2014. The role of ocean
1207 gateways on cooling climate on long time scales. *Global and Planetary Change* 119, 1–22.

1208 Sluijs, A., Pross, J., Brinkhuis, H., 2005. From greenhouse to icehouse; organic-walled dinoflagellate
1209 cysts as paleoenvironmental indicators in the Paleogene. *Earth-Science Reviews* 68, 281–
1210 315.

1211 Spicer, R.A., Harris, N.B.W., Widdowson, M., Herman, A.B., Guo, S., Valdes, P.J., Wolfe, J.A., Kelley,
1212 S.P., 2003. Constant elevation of Southern Tibet over the past 15 million years. *Nature* 412,
1213 622–624.

1214 Stap, L. B., van de Wal, R.S.W., De Boer, B., Bintanja, R., Lourens, L.J., 2016. The MMCO-EOT
1215 conundrum: Same benthic $\delta^{18}\text{O}$, different CO_2 . *Paleoceanography* 31, 1270–1282.

1216 Stein, R., Fahl, K., Schreck, M., Knorr, G., Niessen, F., Forwick, M., Gebhardt, C., Jensen, L., Kaminski,
1217 M., Kopf, A., Matthiessen, J., Jokat, W., Lohmann, G., 2016. Evidence for ice-free summers in
1218 the late Miocene central Arctic Ocean. *Nature Communications* 7, 11148.

1219 Steppuhn, A., Micheels, A., Geiger, G., Mosbrugger, V., 2006. Reconstructing the Late Miocene
1220 climate and oceanic heat flux using the AGCM ECHAM4 coupled to a mixed-layer ocean
1221 model with adjusted flux correction. *Palaeogeography, Palaeoclimatology, Palaeoecology*
1222 238, 399–423.

1223 Taylor, F.J.R., Hoppenrath, M., Saldarriaga, J.F., 2008. Dinoflagellate diversity and distribution.
1224 *Biodiversity and Conservation* 17, 407–418.

1225 Tzanova, A., Herbert, T.D., Peterson, L., 2015. Cooling Mediterranean Sea surface temperatures
1226 during the Late Miocene provide a climate context for evolutionary transitions in Africa and
1227 Eurasia. *Earth and Planetary Science Letters* 419, 71–80.

1228 Utescher, T., Bondarenko, O.V., Mosbrugger, V., 2015. The Cenozoic Cooling – continental signals
1229 from the Atlantic and Pacific side of Eurasia. *Earth and Planetary Science Letters* 415, 121–
1230 133.

1231 Versteegh, G.J., Blokker, P., Bogus, K.A., Harding, I.C., Lewis, J., Oltmanns, S., Rochon, A., Zonneveld,
1232 K.A., 2012. Infra red spectroscopy, flash pyrolysis, thermally assisted hydrolysis and

1233 methylation (THM) in the presence of tetramethylammonium hydroxide (TMAH) of cultured
1234 and sediment-derived *Lingulodinium polyedrum* (Dinoflagellata) cyst walls. Organic
1235 Geochemistry 43, 92–102.

1236 Verhoeven, K., Louwye, S., 2013. Palaeoenvironmental reconstruction and biostratigraphy with
1237 marine palynomorphs of the Plio–Pleistocene in Tjörnes, Northern Iceland.
1238 Palaeogeography, Palaeoclimatology, Palaeoecology 376, 224–243.

1239 Verleye, T.J., Louwye, S., 2010. Recent geographical distribution of organic-walled dinoflagellate
1240 cysts in the southeast Pacific (25–53 S) and their relation to the prevailing hydrographical
1241 conditions. Palaeogeography, Palaeoclimatology, Palaeoecology 298, 319–340.

1242 Versteegh, G.J., Zonneveld, K.A., 1994. Determination of (palaeo-) ecological preferences of
1243 dinoflagellates by applying detrended and canonical correspondence analysis to Late
1244 Pliocene dinoflagellate cyst assemblages of the south Italian Singa section. Review of
1245 Palaeobotany and Palynology 84, 181–199.

1246 von Hagke, C., Oncken, O., Ortner, H., Cederbom, C.E., Aichholzer, S., 2014. Late Miocene to present
1247 deformation and erosion of the Central Alps — Evidence for steady state mountain building
1248 from thermokinematic data. Tectonophysics 632, 250–260.

1249 Warny, S., Askin, R.A., Hannah, M.J., Mohr, B.A., Raine, J.I., Harwood, D.M., Florindo, F., 2009.
1250 Palynomorphs from a sediment core reveal a sudden remarkably warm Antarctica during the
1251 middle Miocene. Geology 37, 955–958.

1252 Wijnker, E., Bor, T., Wesselingh, F., Munsterman, D., Brinkhuis, H., Burger, A., Vonhof, H., Post, K.,
1253 Hoedemakers, K., Janse, A., 2008. Neogene stratigraphy of the Langenboom locality (Noord-
1254 Brabant, the Netherlands). Netherlands Journal of Geosciences-Geologie en Mijnbouw 87,
1255 165–180.

1256 Williams, G.L., Fensome, R.A. and MacRae, R.A., 2017. The Lentin and Williams index of fossil
1257 dinoflagellates. 2017 edition. American Association of Stratigraphic Palynologists
1258 Contributions Series 48, 1097 p.

- 1259 Williams, M., Haywood, A.M., Taylor, S.P., Valdes, P.J., Sellwood, B.W., Hillenbrand, C.-D., 2005.
 1260 Evaluating the efficacy of planktonic foraminifer calcite $\delta^{18}\text{O}$ data for sea surface
 1261 temperature reconstruction for the Late Miocene. *Geobios* 38, 843–863.
- 1262 Wilson, D.S., Pollard, D., Deconto, R.M., Jamieson, S.S., Luyendyk, B.P., 2013. Initiation of the West
 1263 Antarctic Ice Sheet and estimates of total Antarctic ice volume in the earliest Oligocene.
 1264 *Geophysical Research Letters* 40, 4305–4309.
- 1265 Woods, M.A., Vandenbroucke, T.R., Williams, M., Riding, J.B., De Schepper, S., Sabbe, K., 2014.
 1266 Complex response of dinoflagellate cyst distribution patterns to cooler early Oligocene
 1267 oceans. *Earth-Science Reviews* 138, 215–230.
- 1268 Wright, J.D., Miller, K.G., Fairbanks, R.G., 1992. Early and middle Miocene stable isotopes:
 1269 implications for deepwater circulation and climate. *Paleoceanography* 7, 357–389.
- 1270 You, Y., Huber, M., Müller, R., Poulsen, C., Ribbe, J., 2009. Simulation of the middle Miocene climate
 1271 optimum. *Geophysical Research Letters* 36, doi: 10.1029/2008GL036571.
- 1272 Zachos, J., Pagani, M., Sloan, L., Thomas, E., Billups, K., 2001. Trends, rhythms, and aberrations in
 1273 global climate 65 Ma to present. *Science* 292, 686–693.
- 1274 Zachos, J.C., Dickens, G.R., Zeebe, R.E., 2008. An early Cenozoic perspective on greenhouse warming
 1275 and carbon-cycle dynamics. *Nature* 451, 279–283.
- 1276 Zhang, Y.G., Pagani, M., Liu, Z., Bohaty, S.M., DeConto, R., 2013. A 40-million-year history of
 1277 atmospheric CO_2 . *Philosophical Transactions of the Royal Society of London A:*
 1278 *Mathematical, Physical and Engineering Sciences* 371.
- 1279 Zonneveld, K.A., Brummer, G.A., 2000. (Palaeo-) ecological significance, transport and preservation
 1280 of organic-walled dinoflagellate cysts in the Somali Basin, NW Arabian Sea. *Deep Sea*
 1281 *Research Part II: Topical Studies in Oceanography* 47, 2229–2256.
- 1282 Zonneveld, K.A., Marret, F., Versteegh, G. J., Bogus, K., Bonnet, S., Bouimetarhan, I., Crouch, E., De
 1283 Vernal, A., Elshanawany, R., Edwards, L., 2013a. Atlas of modern dinoflagellate cyst
 1284 distribution based on 2405 data points. *Review of Palaeobotany and Palynology* 191, 1–197.

1285 Zonneveld, K.A., Versteegh, G.J., De Lange, G.J., 1997. Preservation of organic-walled dinoflagellate
 1286 cysts in different oxygen regimes: a 10,000 year natural experiment. *Marine*
 1287 *Micropaleontology* 29, 393–405.

1288 Zonneveld, K.A.F.; Versteegh, G.J.M., De Lange, G.J., 2001. Palaeoproductivity and post-depositional
 1289 aerobic organic matter decay reflected by dinoflagellate cyst assemblages of the Eastern
 1290 Mediterranean S1 sapropel. *Marine Geology*, 172, 181–195.

1291 Zonneveld, K.A.F., Marret, F., Versteegh, G.J., Bogus, K., Bonnet, S., Bouimetarhan, I., Crouch, E., De
 1292 Vernal, A., Elshanawany, R., Edwards, L., Esper, O., Forke, S., Grøsfjeld, K., Henry, M.,
 1293 Holzwarth, U., Kieft, J.-F., Kim, S.-Y., Ladouceur, S., Ledu, D., Chen, L., Limoges, A., Londeix, L.,
 1294 Lu, S.-H., Mahmoud, M.S., Marino, G., Matsouka, K., Matthiessen, J., Mildenhall, D.C.,
 1295 Mudie, P.J., Neil, H.L., Pospelova, V., Qi, Y., Radi, T., Richerol, T., Rochon, A., Sangiorgi, F.,
 1296 Solignac, S., Turon, J.-L., Verleye, T., Wang, Y., Wang, Z., Young, M., 2013b. Geographic
 1297 distribution of dinoflagellate cysts in surface sediments, doi: 10.1594/PANGAEA.818280
 1298